

PARTICLE SHAPE AND PARTICLE ORIENTATION IN THE LASER DIFFRACTION AND STATIC IMAGE ANALYSIS SIZE DISTRIBUTION ANALYSIS OF MICROMETER SIZE RECTANGULAR PARTICLES

A.P. Tinke¹, A. Carnicer², R. Govoreanu¹, G. Scheltjens³, L. Lauwerysen¹, N. Mertens¹, K. Vanhoutte¹, and M.E. Brewster¹.

¹ Johnson & Johnson Pharmaceutical Research and Development, Department for Pharmaceutical Development, Pharmaceutical Sciences, Turnhoutseweg 30, B-2340 Beerse, Belgium. Tel. +32 14 607296; Fax +32 14 607083; e-mail: atinke@prdbe.jnj.com.

² University of Barcelona, Department for Applied Physics and Optics, Marti i Franques 1, 08028 Barcelona, Spain. e-mail: artur.carnicer@ub.edu; <http://www.ub.edu/optics>.

³ Karel de Grote-Hogeschool, Campus Hoboken, Industrial Sciences and Technology, Salesianenlaan 30, 2660 Hoboken, Belgium.

ABSTRACT

A systematic study has been described on the laser diffraction (LD) and static image analysis (SIA) of rectangular particles [1]. To rule out powder sampling, sample dispersion and particle orientation as a possible root cause for differences in size distribution profile, powder samples were initially immobilized by means of a dry disperser onto a glass plate. For a defined region of the glass plate the diffraction pattern as induced by the dispersed particles, and the 2D dimensions of the individual particles were measured by LD and optical microscopy, respectively. Correlation between LD and SIA could be demonstrated considering the scattering intensity of the individual particles as the most dominating factor. For both spherical and rectangular particles, theory explains the latter to relate to the square of their projected area. In traditional LD, the size distribution profile is dominated by the maximum projected area of the particles (A), and the diffraction diameters of a rectangular particle with length L and breadth B are perceived by the LD instrument to correspond by approximation with spheres having a diameter of \varnothing_L and \varnothing_B , respectively. Weighting for differences in scattering intensity between spherical and

rectangular particles explains each rectangular particle to contribute to the overall LD volume probability distribution proportional to A^2/L and A^2/B . Accordingly, for rectangular particles this scattering intensity weighted diffraction diameter (SIWDD) concept explains an overestimation of their shortest dimension and an underestimation of their longest dimension. **For this study various samples have been analysed with the longest dimension of the particles ranging from ca. 10 to 1000 μm .** For a variety of pharmaceutical powders all with a different rectangular particle size and shape, the demonstrated correlation between LD and SIA aims to facilitate the user in a better validation of LD methods based on SIA data.

Keywords: Laser Diffraction, Static Image Analysis, Rectangular Particles, Particle Shape, Particle Orientation, Particle Size Distribution, Scattering Intensity Weighted Diffraction Diameter

INTRODUCTION

In the evaluation of pharmaceutical product quality, particulate system characteristics are generally of great concern [2]. To characterize the particle size distribution (PSD) of a pharmaceutical product, a large number of analytical technologies are commercially available. Their capacity to generate reliable data highly relates to the criticality of the product [3], and the specific size (distribution) characteristics one would like to know. In practice, within many application areas a consensus has risen over the years regarding the use of certain preferred PSD characterization technologies. The latter quite often is accompanied by an application specific functional terminology. Accordingly, within pharmaceutical industry for the PSD characterization of dry powders amongst various other analytical techniques, laser diffraction (LD) and image analysis (IA) have been demonstrated to be very important [4].

For a few decades LD has been widely accepted as one of the most powerful PSD characterization technologies [5]. In a strict sense, due to its principle of operation LD is not a true particle size (measurement) technique, rather than a particulate system characterization technique. Hence, it is valid to argue that processing of the diffraction pattern of a single non-spherical particle does not lead to one unique size and shape related particle size [6,7]. The latter can readily be understood, since for a non-spherical particle given its diffraction pattern there is not one single spherical particle of which its diffraction pattern is exactly identical. And since in LD the processing of light scattering data is based on the assumption of spherical particles, the theoretical scattering pattern of a distribution of spherical particles is generally found to give the best fit.

In the literature the phenomenon of light scattering is typically described for circular and rectangular apertures. Since according to Babinet's principle the diffraction patterns produced by so-called complementary screens are nearly identical, the same theory by approximation also applies for solid bodies having the same area of projection [8]. For the light scattering of an object, its irradiance distribution function consists of two parts, being an intensity factor and an angular function. While the intensity factor is described to be a function of the square of the projected area of the particle (A^2) [9], the angular function changes with particle shape [10,11]. The scattered light energy generated by the diffraction process traditionally falls on a set of static concentric detectors. The composite diffraction pattern is thereby a function of the scattering angle and of the percentage of the different particles, which scatter light at that given angle. As a next step in the measurement cycle, the various detector signals are processed on the basis of rigorous Mie theory [12]. The latter requires the relative refractive index (RI) [13] and the coefficient of the light absorptivity [14] of the particles to be known. However, for particles much larger than the wavelength of the incident light (λ) and for which RI is much

larger than unity, things may be simplified and data processing can be done by means of Fraunhofer, which actually is a subset of Mie theory.

Though LD has shown to be an extremely powerful PSD technique in terms of its universal applicability, broad dynamic size range, (relatively) low required sample amount, user friendliness, and (high) robustness and precision, for years a serious discussion is going on regarding the suggested limited accuracy of this technology [15,16,17]. Indeed, from a measurement point of view, (a) the limited angular resolution of the detectors, (b) the limited angular scattering information and scatter intensity at a smaller particle size, and (c) the orientation of (non-spherical) particles should be mentioned. Whereas, from a data processing point of view, (a) the assumption of spherical particles, (b) the limitations of the applied algorithms in the deconvolution of the measured scattering data, and (c) the type of curve fitting [18,19] (e.g., Log-normal, Rosin-Rammler or other) are known to affect the reported results of the laser diffractometer.

The basis for quite some discussions regarding the discrepancy between LD and other PSD technologies is related to the irregular shape of the particles. Differences in size distribution profile generated by different PSD technologies are often referred to as an inaccuracy of either one of the methods. However, as Kaye et al. [20] stated “it is becoming increasingly apparent that the discrepancies are, in fact, information on the shape and structure of the fine particles being studied”. To illustrate the latter, in LD small irregularities on the surface of the particles are known to give rise to high angle scattering, which is interpreted by some laser diffractometers as small ‘ghost’ particles. Second, since the measured scatter intensities will be processed by the LD instrument on the basis of an assumed sphericity of the particles, all shapes that significantly differ from spherical may give rise to seriously biased results [21,22]. Finally and third, the scattered light is generally assumed to be averaged over the various orientations of the particles relative to the laser beam [23]. Together

with smoothing of the PSD profile during data processing [24], this orientation averaging is mentioned in literature as an important source for broadening of the PSD [25]. The latter additionally results in an overestimation of the particle size compared to spheres having an equal volume [26]. It has been suggested to compensate for this overestimation in LD, using a somewhat lower value for the particulate RI [27].

Validation of the accuracy of a PSD method may not always be a straightforward thing to do, since for different analytical technologies inconsistent results are readily obtained sometimes even for what initially are expected to be rather ideal samples [28,29,30]. Amongst other regulatory agencies, the United States Pharmacopeia (USP) highly recommends verification of LD methods by means of optical microscopy [31]. From a fundamental point of view this recommendation is only relevant for products with a size of the particles larger than the detection limit of the optical microscope of ca. 1 μm . In practise, due to various limitations of the technology, the dynamic size range in the image analysis of particulate systems typically runs from ca. 5 to 500 μm (though some manufacturers have demonstrated a wider dynamic size range). Despite these limitations, the recommendation as made by the USP reflects the growing opinion within the particle size community that image analysis of grey-scale images is per definition most accurate and should therefore be selected as the preferred orthogonal technology for validation of LD test methods. Unfortunately, the latter is easier said than done, since for non-spherical particles in terms of volume median diameter (d_{v50}) the particle size of a product as measured with LD is often known to be smaller compared to SIA [32,33]. Additionally, the users efforts to validate the accuracy of a LD method is only to a limited extent facilitated by adequate literature dealing with this matter. As an example of the empirical correlation between LD and IA, Li et al. [34] stated that the ratio of volume median sizes (d_{v50}) is roughly equal to the square root of the mean sphericity of the particles

(i.e., $d_{v50_{LD}}/d_{v50_{IA}} \approx \sqrt{S}$). Here, S is equal to $(D_a/D_p)^2$, where D_a and D_p are defined as the equivalent circular area diameter (or Heywood's diameter) and the equivalent circular perimeter diameter, respectively. Though this concept may be applicable in certain cases, from a fundamental point of view it is difficult to defend as a generic approach in the validation of LD by means of IA.

A more fundamental basis for the validation of LD by means of IA lays in the fact, that both in the process of forward light scattering as in the analysis of grey-scale images the instrument response relates to the projected area of the particles [23,25,32,35]. Since in LD the latter varies in function of their orientation, the classic Cauchy theorem explains that the expected projected area of a randomly oriented convex body is one quarter of its total surface area [36,37]. Additionally, Gabas et al. [38] suggested the lowest and highest number weighted diffraction diameter to relate to the minimum and maximum particulate projected area, respectively. In-line with these observations, Matsuyama et al. [39] mentioned that for elongated particles with an aspect ratio of ca. 10 double peaks are observed in the LD PSD profile representing the minor and major diameter of the particles. But as they additionally stated, these double peaks may be eliminated due to random orientation of the particles, and a single LD peak may appear corresponding to the minor diameter of the original particles. In a next attempt to understand the typical PSD's of non-spherical particles, based on the LD analysis of commercial reference shape standards, Kelly et al. [40] recently stated that for a successful correlation between LD and SIA more than one projected area based size descriptor is required. From an empirical point of view they suggested that the LD PSD profile for micrometer particles with an aspect ratio greater than ca. 1.5 is best described based on the use of the projected area-based shortest and longest dimension of the particles [41].

One can speculate, why after more than three decades of LD its fundamental principles in the analysis of non-spherical particles are understood

only to a limited extent. The easiest (but not necessarily the best) explanation for the latter probably is to mention the policy of the LD manufacturers to consider their instrument specific algorithms for data processing as confidential. The widely adopted idea that the end user is thereby not allowed to verify the accuracy of these algorithms, helps to create a general perception of LD as being a ‘black box’ that generates per definition different PSD results depending on the instrument brand and model. For those who tend to share this opinion, the authors would like comment that LD considers particles to be spherical, and accuracy of the algorithms for data processing can be evaluated on the basis of well characterized spherical reference size standards.

If one nevertheless considers to evaluate the performance of LD based on the use of non-spherical particles, probably even more than for spherical particles one should take into account all aspects, which affect the final results. More precisely, one should be aware that depending on the applied analytical methodology differences in PSD may not only be obtained due to differences in the physical fundamentals of detection, but also due to differences in (a) particle shape and (b) particle orientation, (c) sampling efficiency [42,43,44], and/or (d) sample dispersion. Here, the latter may relate to a whole series of phenomena such as particle (a) dispersion, (b) agglomeration, (c) segregation, (d) attrition, and (e) dissolution [45]. So, if ever one would like to make a conclusion regarding the performance of LD in the size distribution analysis of non-spherical particles, at least one should be able to identify the individual contributions of all the above mentioned factors.

In this publication, a systematic study has been described on the LD and SIA analysis of rectangular particles **with a longest dimension roughly ranging from 10 to 1000 μm . Typical examples of rectangular particles are shown in the general chapter on optical microscopy of the United States Pharmacopeia [1].** To obtain a better understanding of only the impact of particle shape on the LD PSD profile, experiments have been performed in which sampling efficiency, sample

dispersion and particle orientation were ruled out as a possible root cause for differences in PSD. For this purpose, powder samples were dispersed by means of a dry disperser onto a glass plate. For a **defined** circular region of the glass plate both the diffraction pattern as induced by the dispersed particles, and the 2D dimensions of the individual particles were measured. In addition, the effect of particle orientation has been investigated by analyzing the majority of these samples by means of wet or dry dispersion LD and/or dynamic image analysis (DIA).

It recently has been suggested, that from a technical point of view for arbitrarily shaped particles it is possible to calculate the equivalent LD pattern from the images of the IA measurement [46]. Though this statement is definitely true, so far none of these algorithms seem to be commercially available. With this paper the authors would like to demonstrate that based on a few basic assumptions, for rectangular particles their response in LD can be fairly well predicted, that is if there are no issues with regard to the sampling or the dispersion of the sample. Thereby, this paper may facilitate a much better evaluation of LD volume probability data based on SIA, and vice versa. As this study primarily focuses on particle shape and particle orientation, a more in depth discussion on the impact of sample dispersion and sampling efficiency on the LD and SIA size distribution analysis of rectangular particles needs further investigation in the future.

MATERIALS AND METHODS

Chemicals

NIST certified DRI-CAL™ nominal 50 µm polystyrene latex (PSL) particle size standard was from Duke Scientific (Palo Alto, CA, USA). Sodium chloride was from Merck (Darmstadt, Germany). Various active pharmaceutical ingredients (API) were from Johnson & Johnson Pharmaceutical Research and Development

(Beerse, Belgium). These API's consisted of irregular rectangular particles, but all differed in terms of their aspect ratio and particle size distribution (see Figure 1).

Scanning Electron Microscopy (SEM)

For the morphology evaluation (see Table 1) of each powder, binary grey-scale images were recorded with an FEI Company model Phenom™ benchtop scanning electron microscope (Hillsboro, OR, USA). For this purpose, a small amount of the product was deposited on a \varnothing 12.5 mm aluminium stub covered with conductive carbon tape. After gold coating of the sample, the backscatter electron (BSE) signal was measured at ca. 5 kV.

Static Image Analysis (SIA)

Dry dispersion of various powder samples onto a ca. 6×10 cm glass plate was done by means of an Ankersmid model PD-10 dry powder disperser (Oosterhout, The Netherlands). SIA analysis of the dispersed particles was done with a Nikon model Eclipse E1000 brightfield optical microscope (Tokyo, Japan), equipped with a Prior Scientific motorized stage (Rockland, MA, USA). A Hamamatsu Photonics model C3077-71 CCD camera was mounted on the microscope for the acquisition of 256 grey level images with a 640×480 pixel-size. Image acquisition, processing and analysis was done with Princeton Gamma-Tech version 1.06.01 Spirit software (Princeton, NJ, USA). After binarization of the images the individual particles were analysed for their projected area (A), length (L), breadth (B) and roughness (R), with the latter defined as the particulate perimeter divided by its convex perimeter. For the information of the reader, a summary has been presented on the number based mean projected area, length and breadth, as well as their standard deviation (see Table 2). However, since in this paper all discussions on the image analysis data are based on a weighting for the estimated volume of the particles, one should be careful in the interpretation of Table 2. For all measured particles the above

mentioned size and shape characteristics were exported to Microsoft Excel © for off-line data processing (further details on this are discussed in the results and discussion section).

Laser Diffraction – Static Mode (LD-SM)

For several samples, the same microscopic glass plate as analysed by SIA was also analysed by means of LD. For this purpose, a Beckman-Coulter model LS13320 laser diffractometer (Fullerton, CA, USA) was equipped with a Micro Liquid Module (MLM) wet dispersion module. However, in function of the dry dispersion experiments, the wet measurement cell was replaced by a home-made glass plate holder. To allow LD analysis of the particles dispersed on the glass plate, a clean glass plate was initially placed in the holder. After alignment of the instrument laser and measurement of the background signal, the glass plate was taken out off the instrument and placed under the vacuum cylinder of the PD-10 dry disperser. After dry dispersion of the powder, the glass plate was positioned back into the laser diffractometer for measurement of the scattering pattern induced by the deposited particles. **Due to the unique positioning of the glass plate in its holder, the region in line with the Fourier lens of the instrument could be defined fairly accurate.** After LD measurement the glass plate was positioned under the optical microscope and a series of grey-scale images was acquired for approximately the same region that was previously hit by the $\varnothing \approx 2$ cm collimated laser beam of the laser diffractometer. **Within this region for particles with a longest dimension of $< ca. 50 \mu m$ a minimum number of 20.000 particles was measured. Though generally more than 20.000 particles were present, due to limitations of the off line data processing with Microsoft Excel © the maximum number of particles was set at ca. 25.000. It is reasonable to state, that for the size distribution of many pharmaceutical powders the geometric standard deviation (GSD) easily varies between 1.5 and 2.0. Based on the ISO 13322-1 Annex A guideline [42] one can calculate that in case of a GSD of 2.0,**

measurement of 20.000 particles allows one to report the mass median diameter (d_{v50}) with a ca. 73% probability within a $\pm 10\%$ relative error. This probability will go up to ca. 100% for a GSD of 1.5 (and 20.000 particles counted). One should therefore conclude, that depending on the width of the PSD comparison of the LD and SIA data is limited to some extent by the capabilities of the methodology. For this reason, the experimental approach as described here was merely considered as a simple analytical tool to evaluate the general trend of the LD size distribution profile in function of SIA.

Laser Diffraction – Dynamic Mode (LD-DM)

Wet and dry dispersion laser diffraction measurements were performed with either a Malvern Instruments model Mastersizer 2000 laser diffractometer (Malvern, UK) in blue light off detection mode, or with a Beckman-Coulter model LS13320 (Fullerton, CA, USA) instrument in PIDS off detection mode. The Mastersizer 2000 was either equipped with a Hydro 2000 wet dispersion module, or with a Scirocco 2000 dry dispersion module. In addition, the LS13320 was either equipped with a Universal Liquid Module (ULM) or a Micro Liquid Module (MLM) wet dispersion module. For each sample, both the dispersion conditions and the optical model were optimized on a case to case basis.

Dynamic Image Analysis (DIA)

Wet dispersion DIA measurements were performed with an Ankersmid model EyeTech dynamic image analyser (Oosterhout, The Netherlands). For this purpose, after wet dispersion of the sample a diluted portion was transferred to a plastic cuvette and placed into the cuvette holder of the instrument. Homogenation of the particles was achieved by means of a magnetic stirrer. The acquired grey-scale images were analysed for all particles in focus, and based on their equivalent circular area diameter (ECAD) a volume weighted size distribution was generated for comparison with SIA and/or LD. Multiple

measurement of the same cuvette was done in order to demonstrate adequate stability of the dispersed particles.

RESULTS AND DISCUSSION

Theoretical Approach

In order to understand the response of LD as a function of rectangular particle shape, the authors have taken as a starting point the scattering distribution functions as described in literature for spherical (1) and rectangular apertures (2), respectively. In these equations, A is the (projected) area of the aperture, λ is the wavelength of the light, k is the wavenumber ($2\pi/\lambda$), f' is the back focal length of the Fourier lens of the LD instrument, $J_1(x)$ is the Bessel function of the first kind of order one, \varnothing is the diameter of the circular aperture, L and B are the length and breadth of the rectangular aperture, whereas x and y are the linear coordinates in the X and Y direction, respectively and r is the radius coordinate (i.e., x , y and r refer to the observation plane).

$$I(r) = \left(\frac{A}{\lambda f'} \right)^2 \left[2 \frac{J_1(k\varnothing r / 2f')}{k\varnothing r / 2f'} \right]^2 \quad (1)$$

$$I(x, y) = \left(\frac{A}{\lambda f'} \right)^2 \text{sinc}^2 \left(\frac{Lx}{\lambda f'} \right) \text{sinc}^2 \left(\frac{By}{\lambda f'} \right) \quad (2)$$

According to (1) and (2) for particles with the same area (A) but with differences in shape, $I_0 = A^2/(\lambda f')^2$ will be equal being the maximum scattering intensity along the z -axis, whereas the angular scattering function will per definition be different (see Figure 2). For an ensemble of rectangular particles, the projected area data as obtained with SIA in combination with (2) allow one to calculate its composite diffraction pattern, and based on the same algorithms

as used in commercial LD equipment one theoretically can calculate the distribution of spherical particles giving rise to the same diffraction pattern as measured with laser diffraction. Though this approach sounds fairly straightforward, due to the fact that these routines are not (yet) commercially available, validation of laser diffraction means of SIA data is generally far from easy.

In order to facilitate the interpretation of LD data, as a first assumption for a powder with a relatively wide size distribution the angular scattering information of the individual particles is expected to disappear under the composite diffraction pattern of the product. For this reason, as a second assumption the full complexity of (1) and (2) is expected not to be a **precondition** in the correct interpretation of the LD and SIA data. More precisely, the authors assumed the angular scattering function of a rectangular particle by far not as relevant as its maximum scattering intensity, the latter being proportional to A^2 . **Since one may argue that the light scattering of a rectangular particle with length L and breadth B is explained by a superposition of the scattering behavior of two spheres with diameter L (\varnothing_L) and B (\varnothing_B),** respectively, each rectangular particle is now expected to contribute to the PSD of the product on the basis of its scattering intensity weighted diffraction diameter (SIWDD). As is schematically explained in Figure 3, this SIWDD takes into account the difference between the actual projected area of a particle (roughly equal to $L \times B$) and the projected area of two spheres corresponding to the diffraction diameters \varnothing_L and \varnothing_B , respectively. Typically, for a rectangular particle its projected area is smaller than the projected area of a sphere with \varnothing_L , but larger than the projected area of a sphere with \varnothing_B . Consequently, LD analysis of rectangular particles is expected to lead to an overestimation of the shortest dimension, whereas it will lead to an underestimation of the largest dimension.

Given a rectangular particle, the number of spherical particles (N) that is perceived by the LD instrument to give rise to the same scattering pattern is illustrated by (3). In LD, size distribution data are generally reported as volume probability data. Multiplication of N with the volume of the spheres now gives (4), and finally (5). In other words, one can argue that the contribution of each rectangular particle to the overall volume distribution of a particulate system is proportional to A^2/L (i.e., for the longest dimension of the particle) and A^2/B (i.e., for the shortest dimension of the particle). An interesting detail here is, that in line with a volume probability distribution the dimensions of both A^2/L and A^2/B are in m^3 . Contrary to the statement of Kelly et al. [41] that in LD the presented volume probability data are, in fact, projected area data, the hypothesis as represented by (5) points into a different direction. More precisely, based on (5) one can argue that the LD analysis of rectangular particles truly leads to a volume distribution, but overestimating the shortest dimension of the particles, and underestimating their longest dimension.

$$N_B \approx \left(\frac{A_{L \times B}}{A_{\emptyset, B}} \right)^2 \text{ and } N_L \approx \left(\frac{A_{L \times B}}{A_{\emptyset, L}} \right)^2 \quad (3)$$

$$V_B \approx N_B \times \frac{4}{3} \pi \left(\frac{B}{2} \right)^3 \text{ and } V_L \approx N_L \times \frac{4}{3} \pi \left(\frac{L}{2} \right)^3 \quad (4)$$

$$V_B \approx \frac{8}{3\pi} \times \frac{A^2}{B} \text{ and } V_L \approx \frac{8}{3\pi} \times \frac{A^2}{L} \quad (5)$$

Particle Shape

By means of dry dispersion onto a glass plate, an ensemble of particles was immobilized for analysis with both LD and SIA. Though for LD analysis the glass plate had to be placed in an upright position, for small particles with a limited volume versus projected surface area ratio the attractive forces to the glass plate were observed to exceed gravity forces, meaning that any manipulation of the glass plate did not cause the particles to fall off. To allow the interaction of a sufficient number of particles with the ca. 2 cm collimated laser beam of the laser diffractometer, initial experiments were done with rather small particles having a size less than ca. 50 μm .

As a proof of principle and to be sure about the validity of the experimental setup, initial experiments were done with NIST certified material, being nominal 50 μm polystyrene latex (PSL) spheres. In Figure 4 the typical wet dispersion LD size distribution profile of the product is shown together with PSD profiles as they were obtained in static mode for the LD and SIA analysis of the PSL spheres immobilized on a glass plate by means of dry dispersion. Since LD requires a relatively high number of particles present on the glass plate, as shown by the SIA measurements dry dispersion typically leads to the presence of a certain amount of touching particles. These touching particles are represented by an second peak at ca. 100 μm for the LD-SM measurement. Though the SIA and LD-SM size distribution profiles do not show a good correspondence with regard to the touching particles, their main peaks match very well. In Table 3 for the main peak of the PSD profile LD-SM and LD-DM show identical results, thereby demonstrating that dry dispersion of particles on a glass plate does not affect the accuracy of the measurement. Nevertheless, as demonstrated here for narrow distributions inadequate dispersion of the product may lead to biased results. However, the pharmaceutical powders as investigated in this study typically have a much broader distribution than the nominal 50 μm NIST certified size standard. **For this reason, a certain degree of incomplete**

dispersion may not necessarily have the same effect on the LD-SM size distribution profile of the product, since the information of any touching particles is more likely diluted under the large signal originating from the well dispersed primary particles.

Incomplete dispersion was indeed observed to some extent for Compound B even at relatively low obscuration values of ca. 2%. Any touching particles will obviously contribute to the overall PSD profile. However, in order to exclude their complex scattering behavior from the data set, as a starting point any touching particles were removed from the SIA data set based on an estimated maximum critical roughness of the particles of 1.2. Accordingly, in Figure 5 for Compound B the LD-SM size distribution profile is presented together with those obtained with SIA-ECAD and SIA-SIWDD. Additional size distribution data are presented in Table 4. The LD-SM data initially suggest a certain bimodality of the product. However, a more detailed investigation of the product by other analytical means did not show this phenomenon. For this reason, this bimodality was considered as an artifact, possibly caused by a combination of the system specific detector geometry, the deposition and orientation of the limited number of particles present on the glass plate, and limitations of the data processing algorithms. The overlay nevertheless demonstrates, that for the SIA data a better correlation with LD is obtained based on the SIWDD of the particles, instead of using the ECAD. Still a few discrepancies exist between LD-SM and SIA-SIWDD, though these are believed not to be in contradiction with the basic hypothesis that the light scattering of rectangular particles is perceived by the LD instrument to result from the length and breadth of the particles, and weighted for their projected area according to A^2/L and A^2/B . The discrepancy between the size distributions curves below ca. 10 μm may result from either imperfections of the LD optical model, or from an inaccurate sizing of the smallest particles by SIA. In addition, at the high end of the size distribution, the presence of only a limited number of large(r) particles

and the criticality of their position and orientation relative to the detector may be difficult to handle for the data processing algorithms of the LD system. Despite these limitations in experimental setup, and despite the small differences in the PSD profiles, for Compound B the SIWDD concept allows a good correlation between LD and SIA.

In Figure 6 for Compound C the overlay is presented of the size distribution profiles as obtained with LD-SM, SIA-ECAD and SIA-SIWDD, respectively. Additional size distribution data are presented in Table 5. In this case both the ECAD and SIWDD lead to an acceptable correlation between LD and SIA, though one may argue that the SIWDD leads to a slightly better match compared to the ECAD. The reason for the SIA-ECAD and SIA-SIWDD size distribution profiles laying so close together, probably is related to the less elongated shape of the particles. That is, if the aspect ratio gets closer to 1 both concepts are expected to lead to comparable results, whereas if the aspect ratio of the particles goes up, they will lead to (more) pronounced differences. The latter is confirmed for Compound D. By means of SEM this product is demonstrated to consist of acicular particles with a relatively large aspect ratio varying between ca. 2 to 10. In Figure 7 at a 4× magnification, SIA-SIWDD now clearly leads to a much better correlation with LD-SM compared to SIA-ECAD (additional size distribution data are presented in Table 6). For Compound D a clear discrepancy is observed at the low end of the size distribution. This effect at a relatively low magnification reflects, in fact, the typical limitations in terms of limited dynamic size range if only one magnification setting of the optical microscope is used. Separate analysis of fine and large particles at a high and low magnification, respectively, typically allows the assessment of the whole size distribution. According to this approach, excellent correlation between LD and SIA is demonstrated by re-analyzing the glass plate with the immobilized particles at a 10× magnification prior to merging the 4× and 10× data sets.

Particle Orientation

A next step in this study is to get a better understanding of the effect of random orientation of the rectangular particles on the LD size distribution profile. In Figure 8 and Table 4 for Compound B the LD and SIA-ECAD (cumulative) size distribution data are presented for the product both in static and dynamic mode. While the response in SIA is related to the maximum projected area of the particles, dynamic image analysis (DIA) demonstrates a clear shift of the size distribution corresponding to a decrease in projected area due to the random orientation of the particles. However, for LD going from static to dynamic mode this shift in size distribution seems to be less pronounced. The same observation has been made in Figure 9 and Table 5 for Compound C. As a result, one apparently has to conclude that in conventional LD the size distribution profile of an ensemble of rectangular particles is dominated by the maximum projected area of the particles. **The latter suggests a certain orientation of the particles in the measurement cell of the instrument. Though this phenomenon is known indeed, it has been demonstrated in literature to depend on the type of instrument, where detector geometry and the type of particles influence the degree of orientation [47].** However, in case of a true random orientation of the particles, scattering information from their third dimension is expected to find its way into the size distribution of the product.

This challenging idea has been investigated in more detail for simple NaCl crystals (i.e., Compound E). As one may expect, these crystals have an aspect ratio for their projected area close to 1. In accordance to what is stated before, Figure 10 and Table 7 demonstrate at the high end of the size distribution that only the SIA-SIWDD data are comparable to the LD-DM size distribution profile. However, LD-DM analysis of the product in silicon oil shows a pronounced difference at the low end of the size distribution, thereby most likely reflecting the third dimension (i.e., thickness) of the crystals. In order to investigate this idea in more detail, the SIA-SIWDD data were reprocessed

assuming all surfaces of the crystals to contribute to the overall scattering pattern. Based on the length (L) and breadth (B) of the maximum projected area, estimation of the thickness (T) potentially enables one to weight all three diffraction diameters L, B and T for the different surfaces (L×B), (L×T) and (B×T). Based on the SIA data set as measured for Compound E, this approach leads to a fairly good correlation between LD and SIA if one chooses the thickness of the crystals to be 0.9× of their breadth. Though it is not possible to verify the thickness of the particles by means of an orthogonal technique, based on the general perception of salt crystals being more or less cubic, a thickness of 0.9×B seems to be not far from the truth.

From the previous results, the SIWDD has been assumed to be the best descriptor to correlate SIA and LD data. Based on the hypothesis that in LD the size distribution of an ensemble of rectangular particles is dominated by the maximum projected area of the particles, whereas with an increasing particle thickness a more pronounced discrepancy will be observed at the low end of the size distribution, experiments have been done with a series of different products in order to evaluate this concept in further detail.

Concept Evaluation

As a first example, in Figure 11 and Table 4 the LD and SIA size distribution data are presented for Compound B. From the SEM images of this product, the particles can be characterized as thin flakes with an aspect ratio ca. 1 to 3. Due to the thin nature of the particles, their third dimension is expected to contribute to the overall scattering profile of the product only to a limited extent. At the high end of the size distribution wet dispersion LD analysis in water leads to an almost identical profile compared to SIA-SIWDD, whereas indeed at the low end of the size distribution only a small deviation arises. Since an inaccurate sizing by the SIA system in this region of the PSD profile seemed unlikely, possible explanations for this deviation (except for the influence of the particle

thickness) could be inadequate dispersion of the fine particles in the case of SIA, or inaccuracy of the optical model in the case of LD. In Figure 12 and Table 5 for Compound C at the high end of the size distribution again LD and SIA show an almost identical profile, whereas at the low end of the size distribution again a difference arises, which is more serious than for Compound B. Based on an excellent fit of the LD size distribution profile illustrated by the weighted residual of 0.125, any biased results were not expected to result from the processing of the light scattering data. A possible explanation for this phenomenon could be the non-representative detection of fine particles by the SIA method related to possible dispersion, detection and/or image analysis issues. Based on SEM analysis of Compound C (see Figure 1) indeed a serious amount of fine particles was observed to be present in the product. Consequently, in SIA an inadequate dispersion of fines could lead to an underestimation at the low end of the PSD. Alternatively, in LD an overestimation of fine particles may occur due to the tendency of the technique to broaden the size distribution of irregular particles [48,49]. However, this broadening at the low end of the PSD may also relate to the contribution of the third dimension of the particles. Based on SEM analysis, the particle thickness for Compound C is seen to be significantly larger compared to Compound B. Therefore, it is not unlikely that a larger thickness of the particles is responsible for a more significant contribution of the third dimension of the particles (of Compound C) to the overall scattering profile. The latter thereby may lead to a more pronounced difference between SIA (which is only a 2D reflection of the particles), and LD (which reflects all 3 dimensions of the particles).

In Figure 13 and Table 8 the SIA and LD size distribution data are shown for Compound F. Since wet dispersion LD initially showed an incomplete dispersion of the particles, based on the excellent correlation as shown in this figure, dry dispersion LD at a low dispersion pressure of only 0.1 bar was believed to reflect much better the LD scattering profile of the primary particles.

In Figure 14 and Table 9 the SIA and LD size distribution data are shown for Compound G. This product is chemically identical to Compound F, but now showing a much broader size distribution due to the presence of more fine and coarse particles. Even for this rather broad size distribution, the SIA-SIWDD size distribution profile corresponds fairly well to the one obtained with LD. At the low end of the size distribution, most definitely with SIA the fine particles below ca. 25 μm are missed at the 2 \times magnification setting of the optical microscope. For this reason in Figure 14B with regard to the cumulative PSD overlay, the LD data were plotted only from $\geq 10 \mu\text{m}$.

The ultimate test is reflected in Figure 15 by the LD and SIA size distribution profiles of Compound H. The particles in this product have a clear lath like structure, and they are characterized by an extremely wide size distribution. For this experiment, the coarse particles were removed from the product by means of a sieve with a cut-off of 250 μm . Since SEM images show the particles to be rather flat, their thickness was expected not to contribute to a serious broadening of the size distribution in LD. For Figure 15A, the PSD overlay again demonstrates an excellent correlation for the SIA-SIWDD data compared to the LD data as obtained with the Malvern Mastersizer 2000 laser diffractometer. The difference at the low end of the size distribution, obviously relates to the limited size range of the SIA system at a 2 \times magnification setting of the optical microscope. Initially, the difference at the high end of the size distribution was believed to relate to either sampling issues in SIA, or to limited capabilities of the laser diffractometer in the accurate sizing of coarse particles above ca. 300 μm . However, a more plausible reason for the slight inconsistency between the SIA and LD data became apparent when only the information on the length (L) of the particles was taken into account (i.e., A^2/L) and plotted in overlay with the LD size distribution data as obtained for the same product by the Beckman-Coulter LS13320 instrument (see Figure 16B). Since a clear correlation was demonstrated between SIA and LD by leaving out the

information on the Breadth (B) of the particles, alignment of the particles in the detection cell of the instrument has been proven to occur. As a result, it seems very likely that for the Beckman-Coulter data the inconsistency between SIA and LD at the left side of the distribution is caused by a certain degree of random orientation for smaller particles. Alternatively, it seems plausible that for the Malvern Instruments data de inconsistency between SIA and LD at the right side of the distribution is caused by a certain degree of alignment for the larger particles. Future studies with other pieces of equipment (i.e., different brands and different models) should demonstrate the extent to which the concept of the SIWDD can be used to evaluate alignment and (random) orientation of non-spherical particles in LD.

CONCLUSIONS

A systematic study has been described on the LD and SIA analysis of rectangular particles, **having different shapes and having a longest dimension ranging from ca. 10 to 1000 μm .** For an ensemble of rectangular particles, their LD size distribution profile appears to be dominated by the maximum projected area (A) of the particles as measured by means of SIA. Moreover, this study has demonstrated that the diffraction diameters of a rectangular particle with length L and breadth B are perceived by the LD instrument to correspond by approximation with spheres having a diameter of \varnothing_L and \varnothing_B , respectively. **The equivalent circular area diameter (ECAD) is traditionally used in the comparison of LD and SIA data.** However, based on the various examples as shown and discussed in this paper, one has to conclude that for micrometer size rectangular particles the scattering intensity weighted diffraction diameter (SIWDD) is a better basis for the correlation of SIA data with LD. Here, weighting for differences in the estimated scattering intensity between spherical and rectangular particles explains randomly orientated rectangular particles to contribute to the overall LD volume probability distribution proportional to A^2/L

and A^2/B . Alternatively, for particles that show a certain degree of alignment, information on L and B need a different interpretation. An example has been shown, where the overall LD volume probability distribution is proportional primarily to A^2/L .

The data as discussed in this paper allow the user to interpret the LD PSD data much more in function of the size and shape of the particles. For this purpose, cumulative undersize data (i.e., d_v10 , d_v50 and d_v90) are less informative than an overlay of the size distribution profiles. Whether cumulative or differential size distribution data are most suitable for correlating LD and SIA very much depends on the characteristics of the product, and the capabilities of the applied methods. In traditional LD, for randomly oriented rectangular particles were A^2/L and A^2/B both need to be taken into account, the SIWDD concept explains an overestimation of the shortest dimension and an underestimation of the longest dimension of the particles.

Based on the data as discussed in this paper, differences in size distribution profile for different pieces of LD equipment seem to relate less to the general perception of LD as being a black box. Correlation of LD and SIA as explained here, offers a new analytical tool that potentially allows an evaluation of the sampling and dispersion efficiency of either of the two methods. Thereby, this study aims to contribute to a much better validation of LD methods by means of SIA.

ABBREVIATIONS

σ	-	standard deviation
A	-	maximum projected area of rectangular particle
AR	-	aspect ratio
B	-	breadth of rectangular particle
DIA	-	dynamic image analysis
DM	-	dynamic mode

ECAD	-	equivalent circular area diameter
IA	-	image analysis
L	-	length of rectangular particle
LD	-	laser diffraction
PSD	-	particle size distribution
R	-	particle roughness
RI	-	refractive index
SEM	-	scanning electron microscopy
SIA	-	static image analysis
SIWDD	-	scattering intensity weighted diffraction diameter
SM	-	static mode
Span	-	$(d_{90} - d_{10})/d_{50}$

ACKNOWLEDGEMENTS

The authors would like to thank Eddy Heyns from the Scientific Instrument Development department (Janssen Pharmaceutica, Beerse, Belgium) for making the glass plate holders that have been used in this study. Johan Verhoeven from the department for Analytical Development needs to be mentioned for making the Excel-template containing the macro's for processing of the static image analysis data.

TABLES AND FIGURES

Table 1

Identification of the various products (i.e., Compound A, B, C, D, E, F, G and H) that have been investigated in this study.

Compound	Morphology (*)	Length (#)	AR (Δ)
A	Equant (spherical)	50	1
B	Flake	10 – 30	1 – 3
C	Plate	10 – 50	1 – 4
D	Acicular	25 – 250	2 – 10
E	Equant (cubical)	100 – 300	1 – 1.5
F	Plate	50 – 150	2 – 3
G	Plate	20 – 200	1 – 3
H	Lath	50 – 500	2 – 5

(*) - Morphology evaluation according to the United States Pharmacopeia [1] based on SEM images.

(#) - Estimation of the longest dimension (μm) based on SEM images of the sample material.

(Δ) - Estimation of the aspect ratio based on SEM images of the sample material.

Table 2

Static image analysis characterization of the various product samples (i.e., Compound A, B, C, D, E, F, G and H) in terms of their number based mean projected area, length and breadth, as well as their standard deviation.

Compound	Area (μm^2)		Length (μm)		Breadth (μm)	
	Mean	St.Dev.	Mean	St.Dev.	Mean	St.Dev.
A	824	1281	27	27	23	22
B	129	155	20	12	9	6
C	67	96	11	7	7	4
D (*)	395	649	32	26	16	10
E	10609	16363	121	94	87	77
F	1348	2868	40	43	27	26
G	1739	3386	53	35	37	24
H	3704	5260	94	60	51	30

(*) - The means and standard deviations have been reported for the SIA data set obtained at a 4 \times magnification.

Table 3

For a nominal 50 μm polystyrene latex standard (i.e., Compound A) the LD size distribution data as measured with a Beckman-Coulter LS13320 laser diffractometer in dynamic mode (LD-DM) and static mode (LD-SM) are compared with the certificate of analysis of the material.

50 μm PSL (*)	\varnothing (μm)	σ (μm)	d_{v10} (μm)	d_{v90} (μm)
Certificate	49.7 ± 2.0	3.4	n.a.	n.a.
LD-DM	50.0	3.8	44.7	55.8
LD-SM (*)	50.2	3.7	44.9	55.8

(*) - Statistical descriptors have been calculated for the main peak of the PSD.

Table 4

The d_{v10} , d_{v50} and d_{v90} cumulative undersize and the span have been calculated for the PSD of Compound B analysed by means of the various LD and IA methodologies.

	d_{v10} (μm)	d_{v50} (μm)	d_{v90} (μm)	Span
LD-SM	5.7	14.1	36.4	2.17
LD-DM (*)	6.2	14.3	31.9	1.80
LD-DM (#)	6.0	14.0	32.1	1.86
SIA-ECAD	9.7	17.0	27.7	1.06
DIA-ECAD	9.5	15.6	25.1	1.00
SIA-SIWDD	7.5	14.7	35.4	1.90

(*) - measurements with Beckman-Coulter LS13320 laser diffractometer

(#) - measurements with Malvern Instruments Mastersizer 2000

Table 5

The d_{v10} , d_{v50} and d_{v90} cumulative undersize and the span have been calculated for the PSD of Compound C analysed by means of the various LD and SIA methodologies.

	d_{v10} (μm)	d_{v50} (μm)	d_{v90} (μm)	Span
LD-SM	6.2	12.7	27.8	1.70
LD-DM (*)	6.8	14.6	29.5	1.55
LD-DM (#)	6.1	14.1	29.9	1.69
SIA-ECAD	8.0	17.0	27.6	1.15
SIA-SIWDD	7.4	16.4	34.6	1.66

(*) - measurements with Beckman-Coulter LS13320 laser diffractometer

(#) - measurements with Malvern Instruments Mastersizer 2000

Table 6

The d_{v10} , d_{v50} and d_{v90} cumulative undersize and the span have been calculated for the PSD of Compound D analysed by means of the various LD and SIA methodologies.

	d_{v10} (μm)	d_{v50} (μm)	d_{v90} (μm)	Span
LD-SM	10.7	30.3	81.2	2.33
SIA-ECAD (*)	18.5	42.1	78.2	1.42
SIA-SIWDD (*)	15.7	34.5	95.4	2.31
SIA-SIWDD (#)	9.9	32.3	88.3	2.43

(*) - microscopy measurement at 4 \times magnification

(#) - microscopy measurement at 4 \times and 10 \times magnification

Table 7

The d_{v10} , d_{v50} and d_{v90} cumulative undersize and the span have been calculated for the PSD of Compound E analysed by means of the various LD and SIA methodologies.

	d_{v10} (μm)	d_{v50} (μm)	d_{v90} (μm)	Span
LD-DM	139	223	351	0.95
SIA-ECAD	147	227	310	0.72
SIA-SIWDD (2D)	153	248	373	0.89
SIA-SIWDD (3D)	140	228	340	0.88

Table 8

The d_{v10} , d_{v50} and d_{v90} cumulative undersize and the span have been calculated for the PSD of Compound F analysed by means of the various LD and SIA methodologies.

	d_{v10} (μm)	d_{v50} (μm)	d_{v90} (μm)	Span
LD-DM	44.9	95.0	177.2	1.39
SIA-ECAD	55.7	98.2	154.1	1.00
SIA-SIWDD	51.6	107.4	192.3	1.31

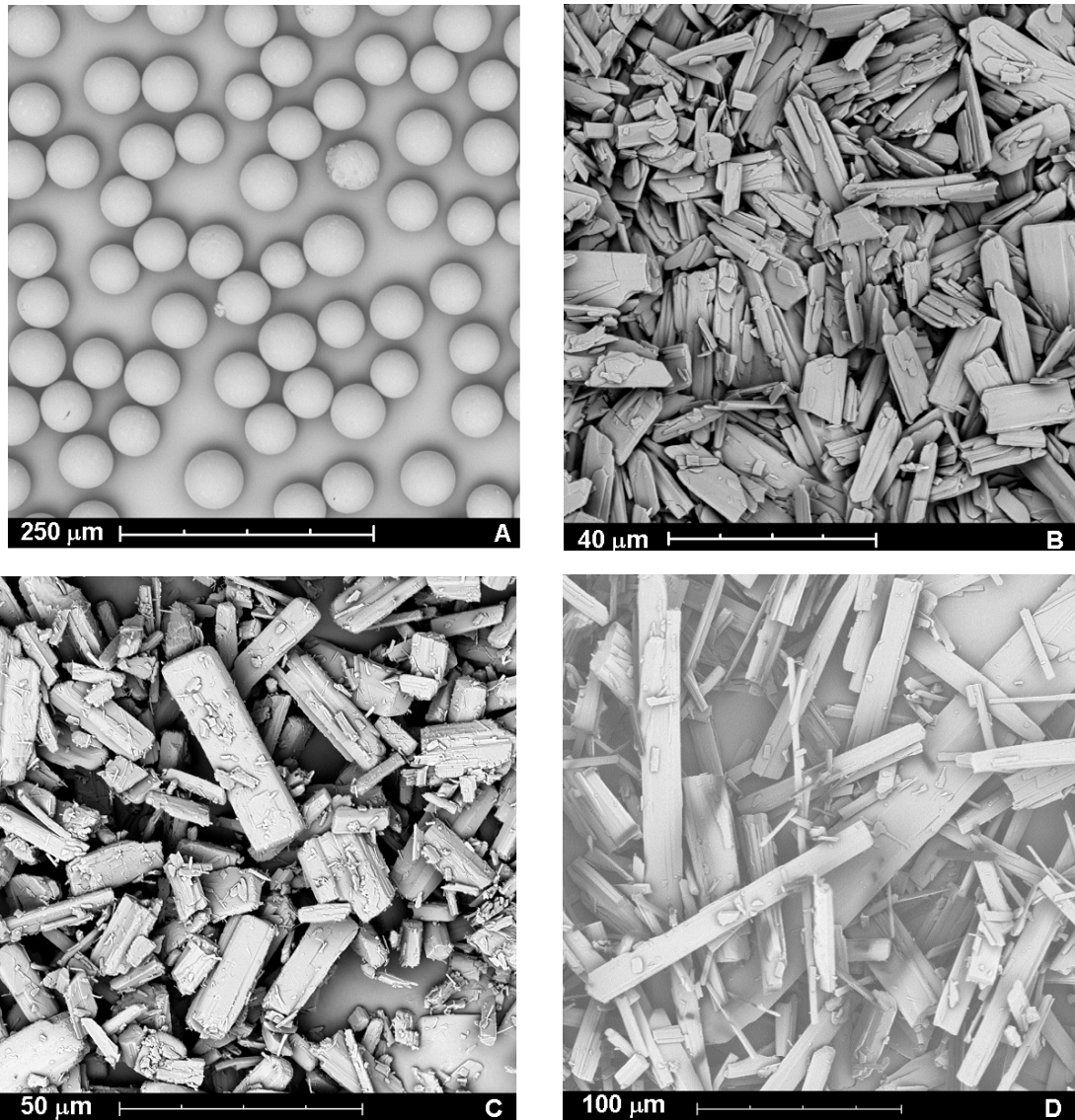
Table 9

The d_{v10} , d_{v50} and d_{v90} cumulative undersize and the span have been calculated for the PSD of Compound G analysed by means of the various LD and SIA methodologies.

	d_{v10} (μm)	d_{v50} (μm)	d_{v90} (μm)	Span
LD-DM	38.0	101.0	246.5	2.06
SIA-ECAD	43.3	95.8	233.8	1.99
SIA-SIWDD	44.4	104.0	281.1	2.28

Figure 1

Representative SEM images of the various products (i.e., Compound A, B, C, D, E, F, G and H) that have been used for this study.



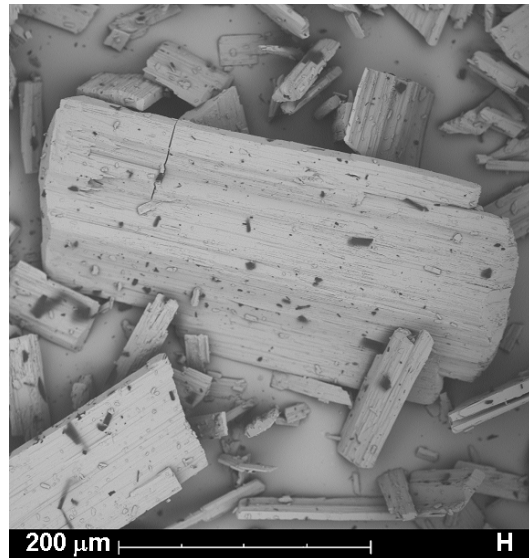
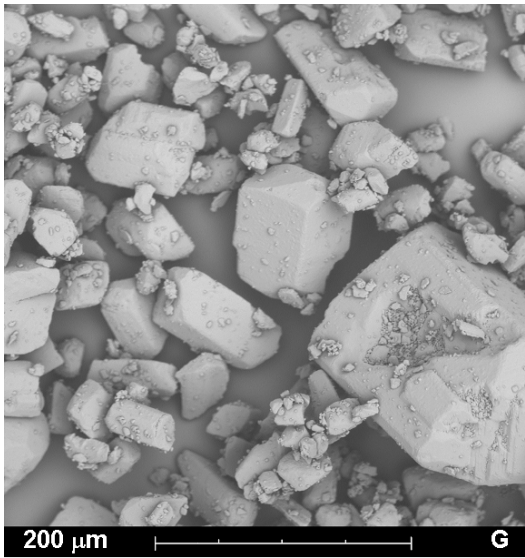
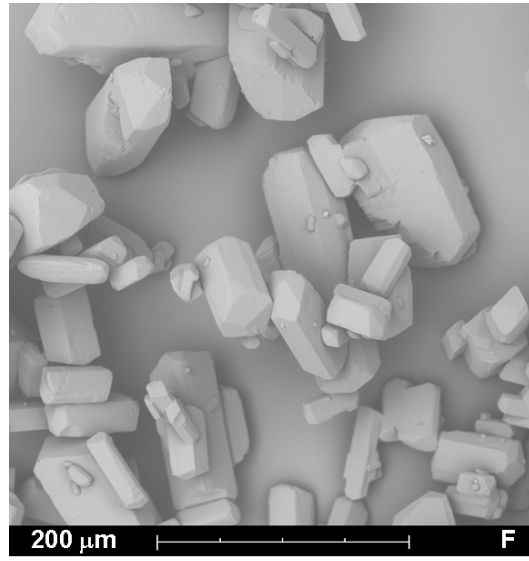
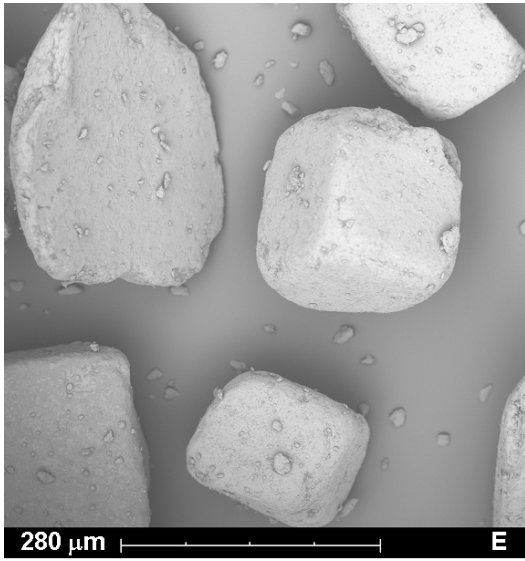


Figure 2

The theoretical scattering patterns for a circular (with $\varnothing = 10 \mu\text{m}$) and a square aperture (with each side being $8.86 \mu\text{m}$) illustrate the fundamental differences in the scatter intensity and angular scattering function for spherical and rectangular particles. These plots have been obtained considering $\lambda = 750 \text{ nm}$.

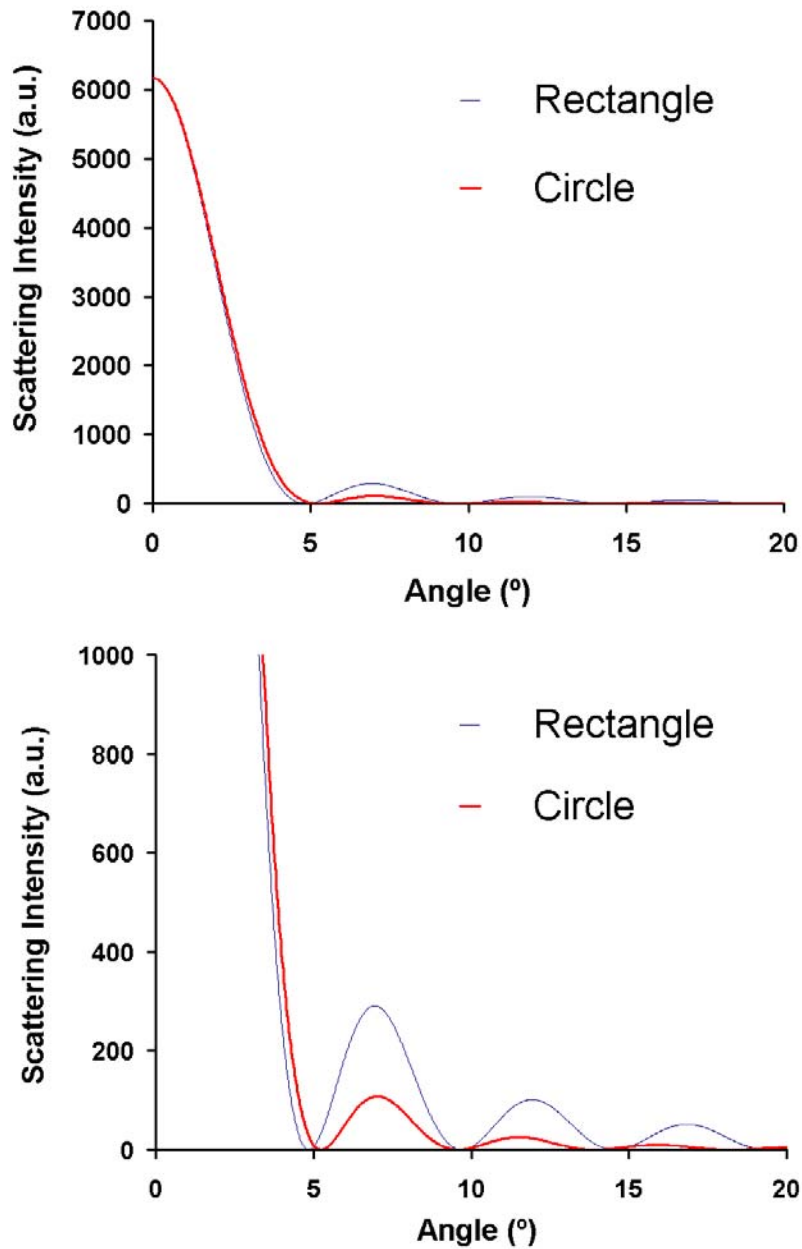


Figure 3

For a rectangular particle the scatter intensity is related to its projected area (A^2), whereas the angular scattering function is determined by both its length (L) and breadth (B).

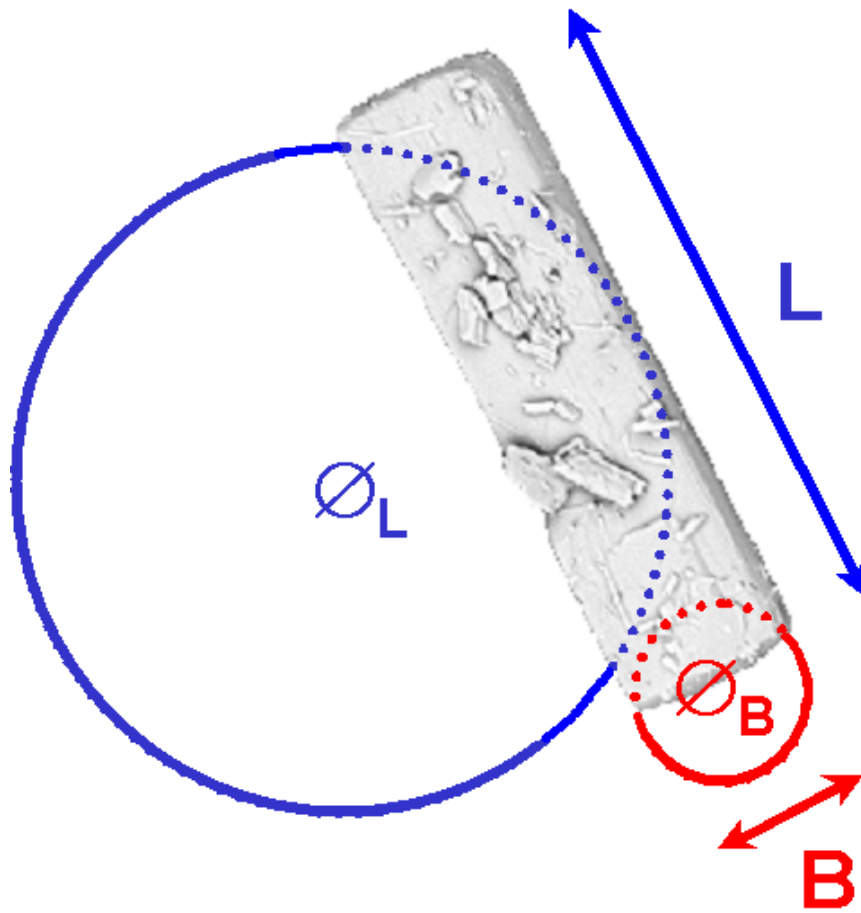


Figure 4

Particle size distribution by volume for a NIST certified nominal 50 μm polystyrene latex standard analysed by means of (LD-DM) laser diffraction and wet dispersion in water, (LD-SM) laser diffraction and dry dispersion on glass plate, and (SIA-ECAD) static image analysis based on the equivalent circular area diameter of the particles.

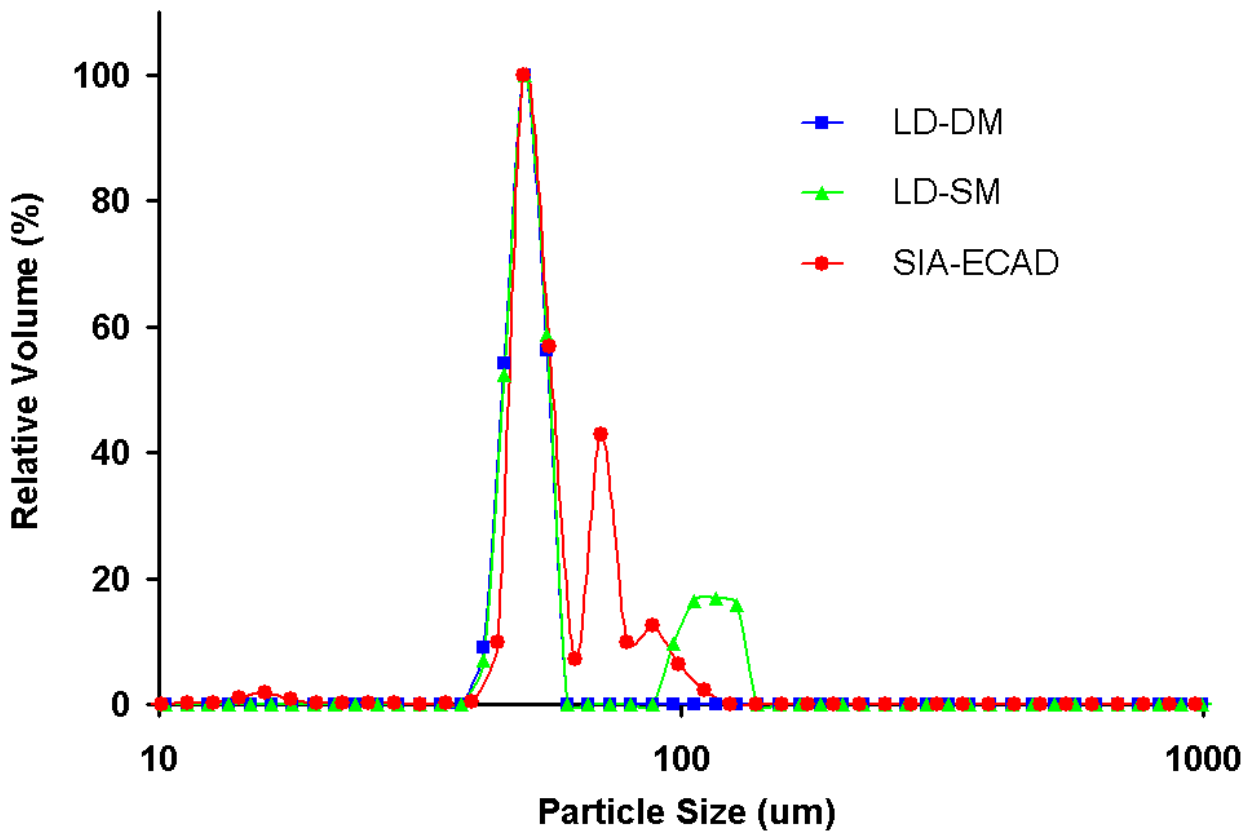


Figure 5

Particle size distribution by volume for the same sample of Compound B analysed by means of (LD-SM) laser diffraction and dry dispersion on glass plate, (SIA-ECAD) static image analysis based on the equivalent circular area diameter of the particles, and (SIA-SIWDD) static image analysis based on the scattering intensity weighted diffraction diameter of the particles.

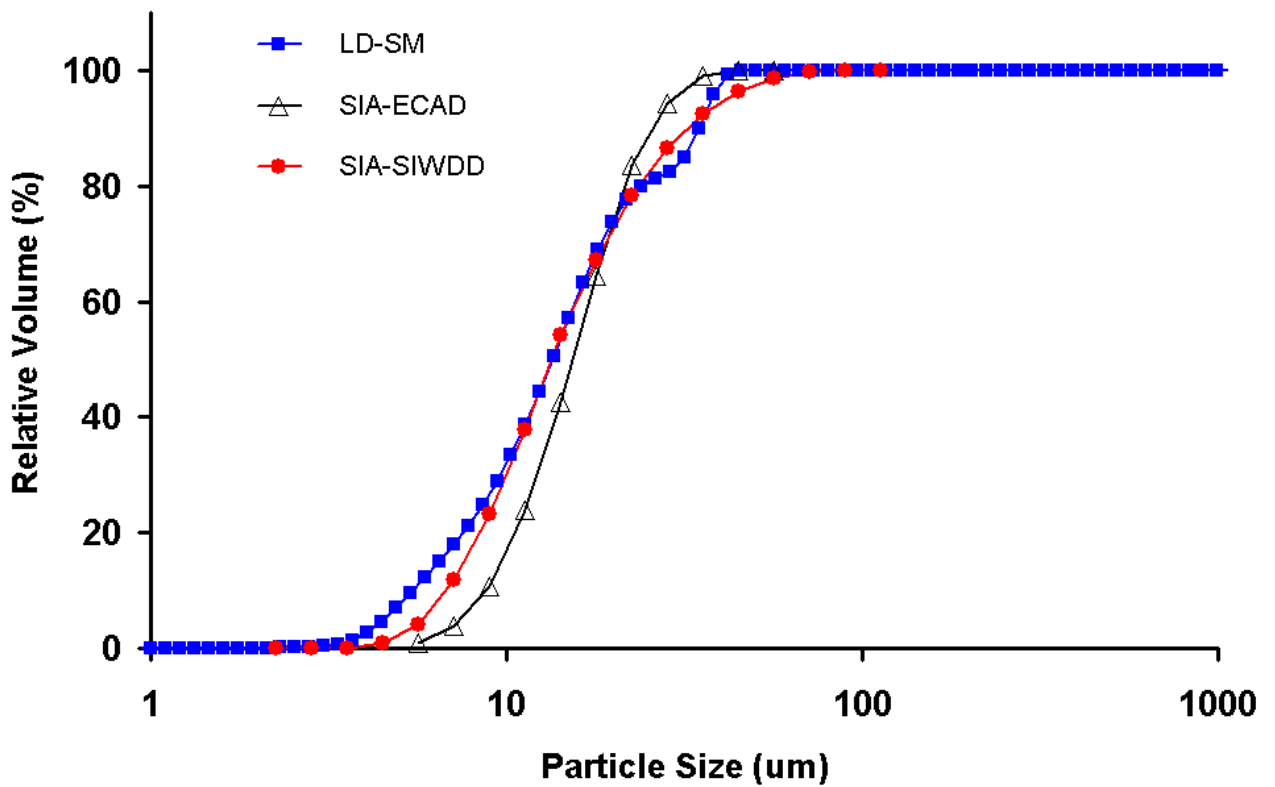


Figure 6

Particle size distribution by volume for the same sample of Compound C analysed by means of (LD-SM) laser diffraction and dry dispersion on glass plate, (SIA-ECAD) static image analysis based on the equivalent circular area diameter of the particles, and (SIA-SIWDD) static image analysis based on the scattering intensity weighted diffraction diameter of the particles.

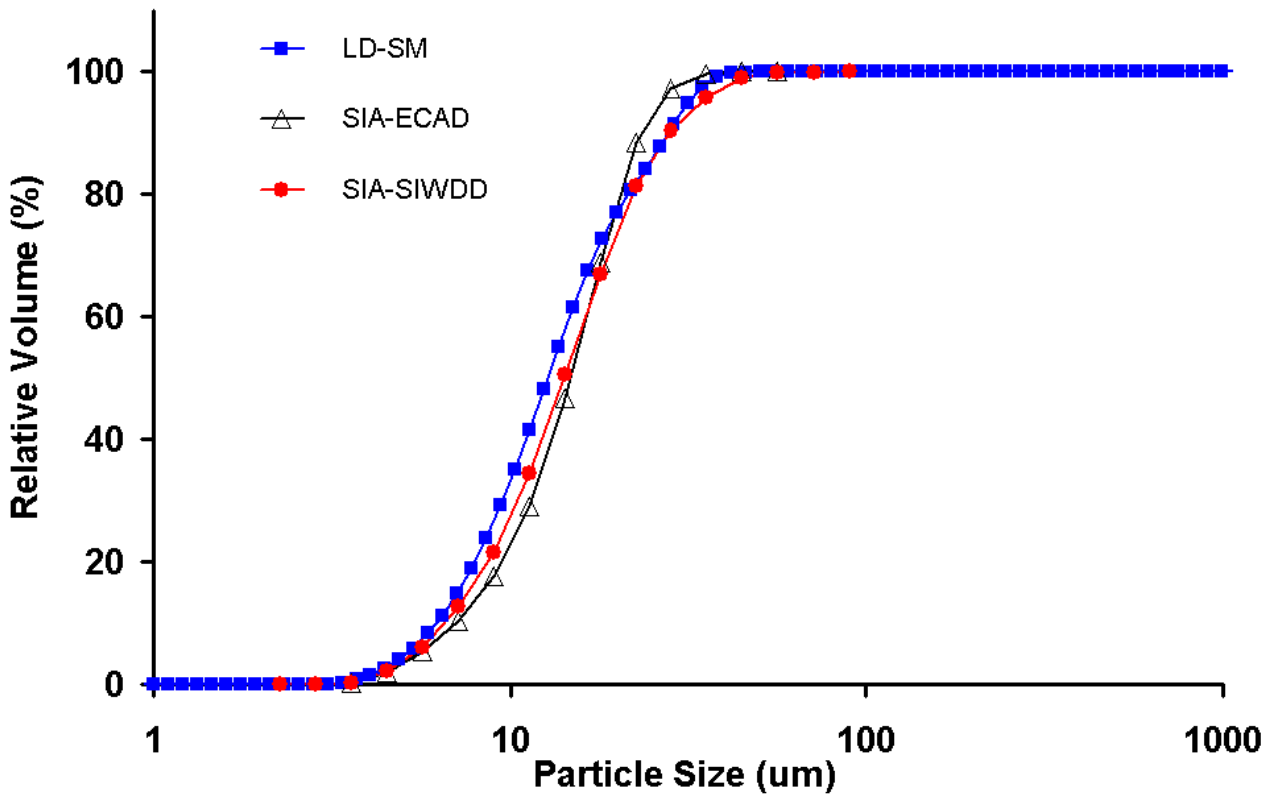


Figure 7

Particle size distribution by volume for the same sample of Compound D analysed by means of (LD-SM) laser diffraction and dry dispersion on glass plate, (SIA-ECAD) static image analysis based on the equivalent circular area diameter of the particles, and (SIA-SIWDD) static image analysis based on the scattering intensity weighted diffraction diameter of the particles (i.e., at 4× magnification and at a combined 4× and 10× magnification).

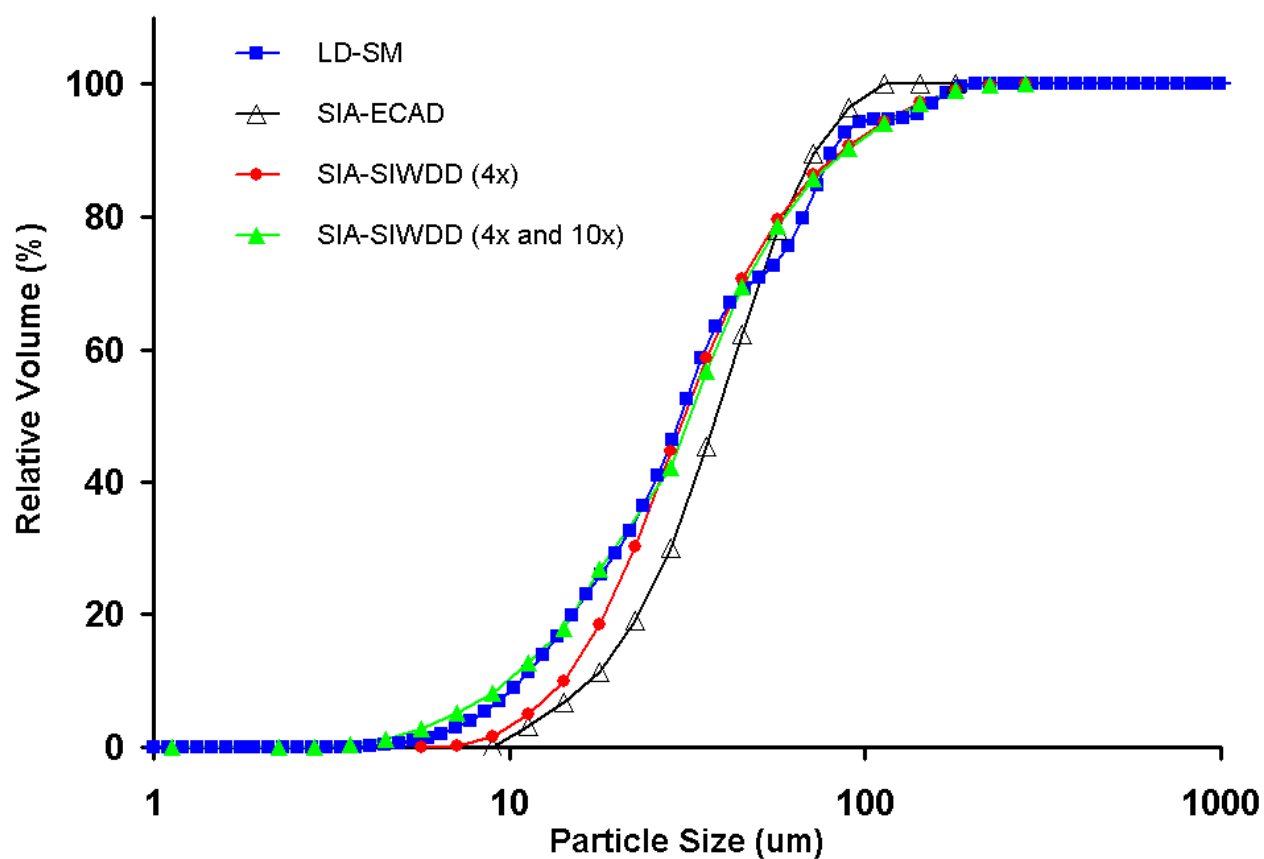


Figure 8

Particle size distribution by volume for Compound B analysed by means of (LD-DM) laser diffraction and wet dispersion in water at an 11% obscuration, (LD-SM) laser diffraction and dry dispersion on glass plate at a 5% obscuration, (SIA-ECAD) static image analysis and dry dispersion on glass plate, and (DIA-ECAD) dynamic image analysis and wet dispersion in water.

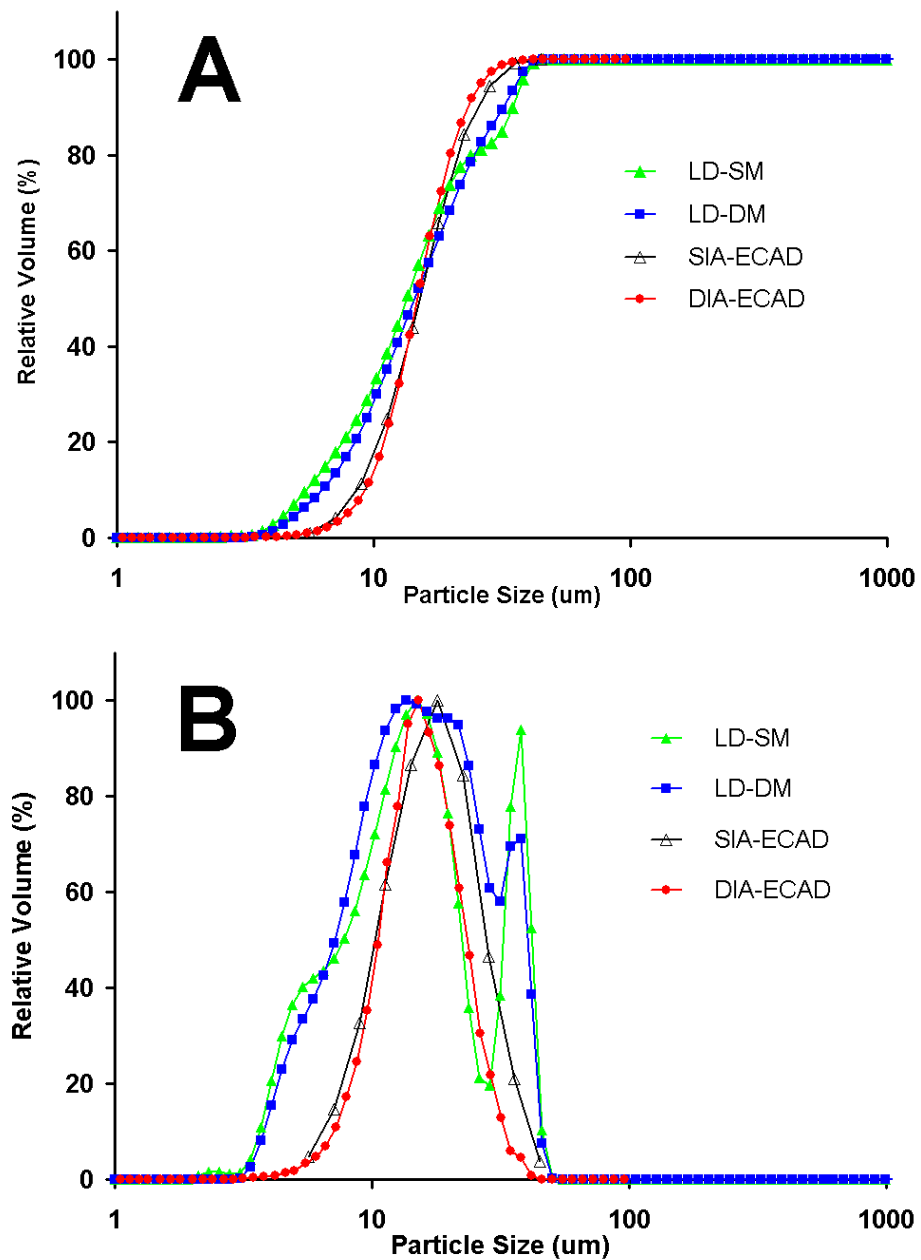


Figure 9

Particle size distribution by volume for Compound C analysed by means of (LD-DM) laser diffraction and wet dispersion in silicon oil at a 8% obscuration, (LD-SM) laser diffraction and dry dispersion on glass plate at a 3% obscuration.

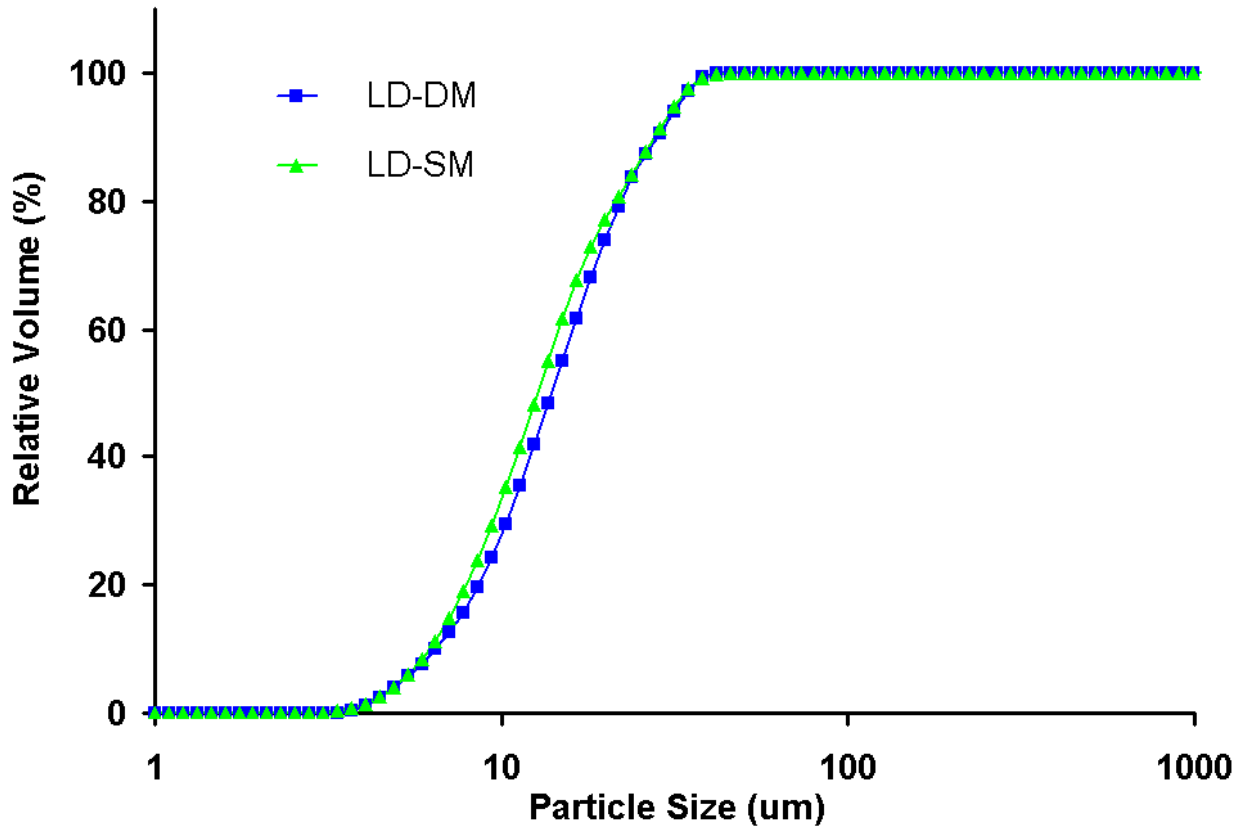


Figure 10

Particle size distribution (PSD) by volume for Compound E analysed by means of (LD-DM) a Malvern Mastersizer 2000 laser diffractometer in combination with a Hydro 2000 wet dispersion module in silicon oil, and (SIA) static image analysis at a $2\times$ magnification and 0.1 bar dispersion pressure, and based on the (SIA-ECAD) equivalent circular area diameter, and (SIA-SIWDD (2D)) scattering intensity weighted diffraction diameter of the particles, respectively. In addition, for (SIA-SIWDD (3D)) based on an estimated thickness of $0.9\times$ the breadth of the particles the theoretical PSD profile has been calculated taking into account the third dimension of the particles.

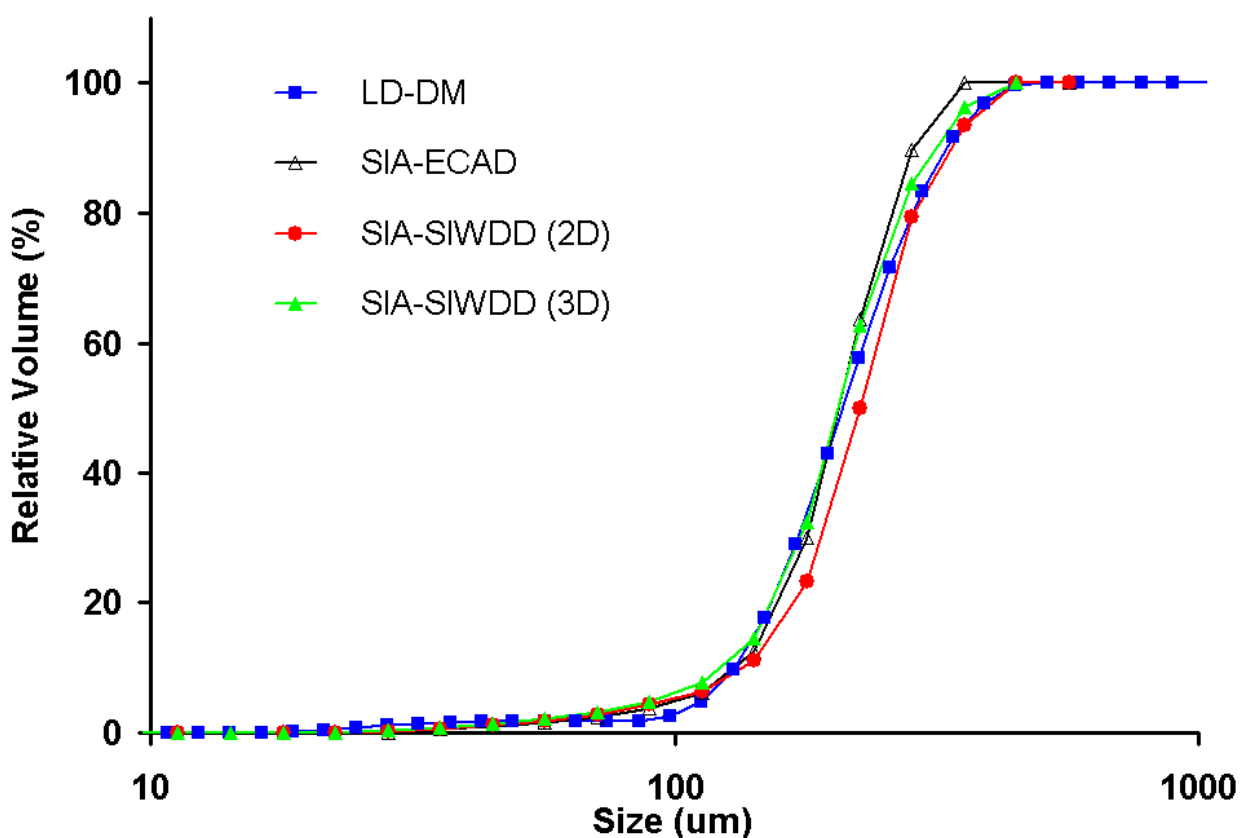


Figure 11

Particle size distribution by volume for Compound B analysed by means of (LD-DM) a Malvern Mastersizer 2000 laser diffractometer in combination with a Hydro 2000 wet dispersion module in water, and static image analysis at a 10× magnification and 0.45 bar dispersion pressure, and based on the (SIA-ECAD) equivalent circular area diameter, and (SIA-SIWDD) scattering intensity weighted diffraction diameter of the particles, respectively.

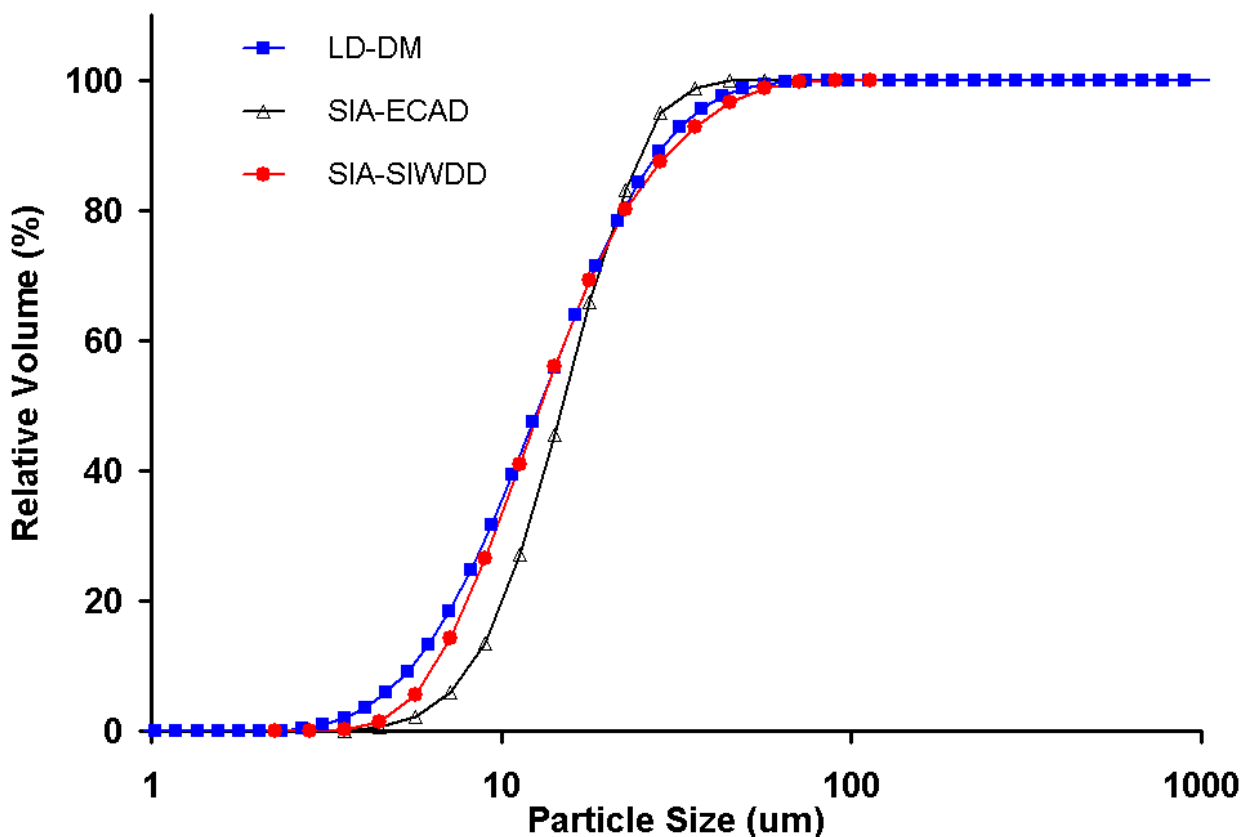


Figure 12

Particle size distribution by volume for Compound C analysed by means of (LD-DM) a Malvern Mastersizer 2000 laser diffractometer in combination with a Hydro 2000 wet dispersion module in silicon oil, and static image analysis at a 10× magnification and 0.3 bar dispersion pressure, and based on the (SIA-ECAD) equivalent circular area diameter, and (SIA-SIWDD) scattering intensity weighted diffraction diameter of the particles, respectively.

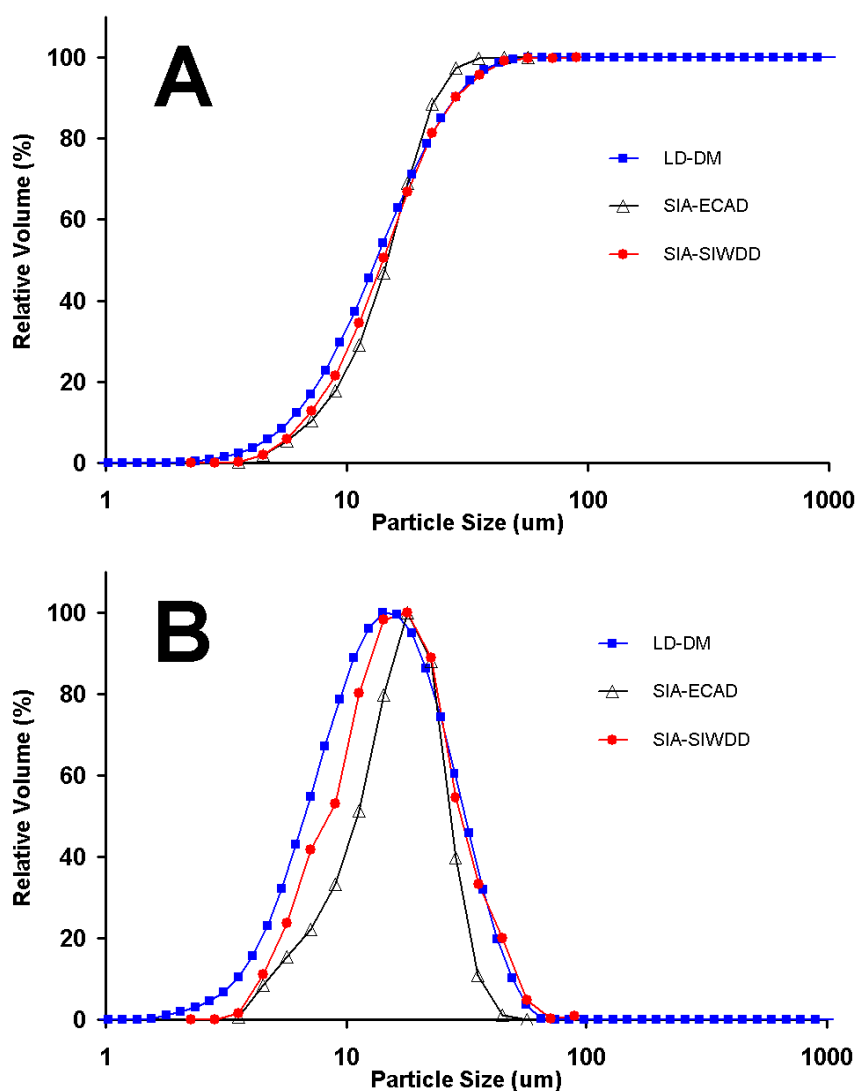


Figure 13

Particle size distribution (PSD) by volume for Compound F analysed by means of (LD-DM) a Malvern Mastersizer 2000 laser diffractometer in combination with a Scirocco 2000 dry dispersion module at 0.1 bar, and static image analysis at a 4× magnification and 0.05 bar dispersion pressure, and based on the (SIA-ECAD) equivalent circular area diameter, and (SIA-SIWDD) scattering intensity weighted diffraction diameter of the particles, respectively.

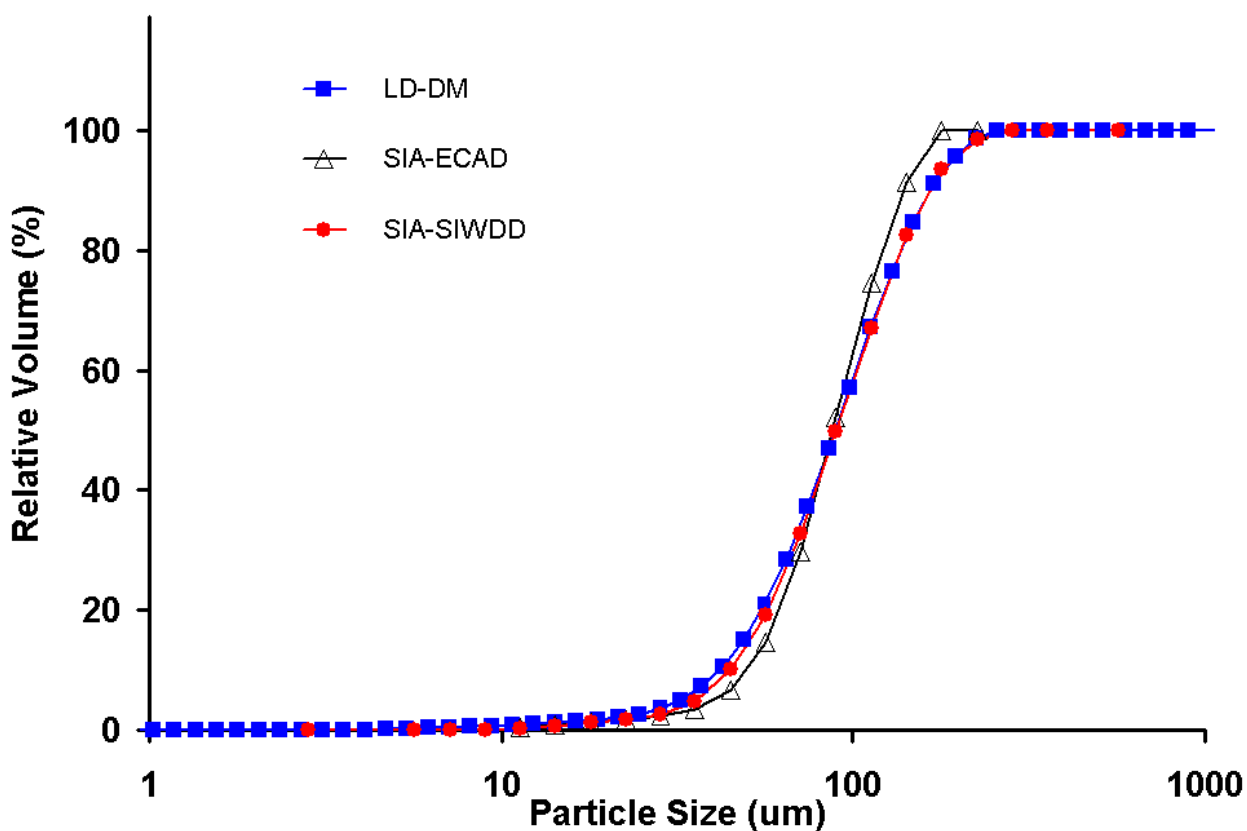


Figure 14

Particle size distribution (PSD) by volume for Compound G analysed by means of (LD-DM) a Malvern Mastersizer 2000 laser diffractometer in combination with a Hydro 2000 wet dispersion module in sunflower oil, and (SIA) static image analysis at a 2× magnification and 0.1 bar dispersion pressure, and based on the (SIA-ECAD) equivalent circular area diameter, and (SIA-SIWDD) scattering intensity weighted diffraction diameter of the particles, respectively.

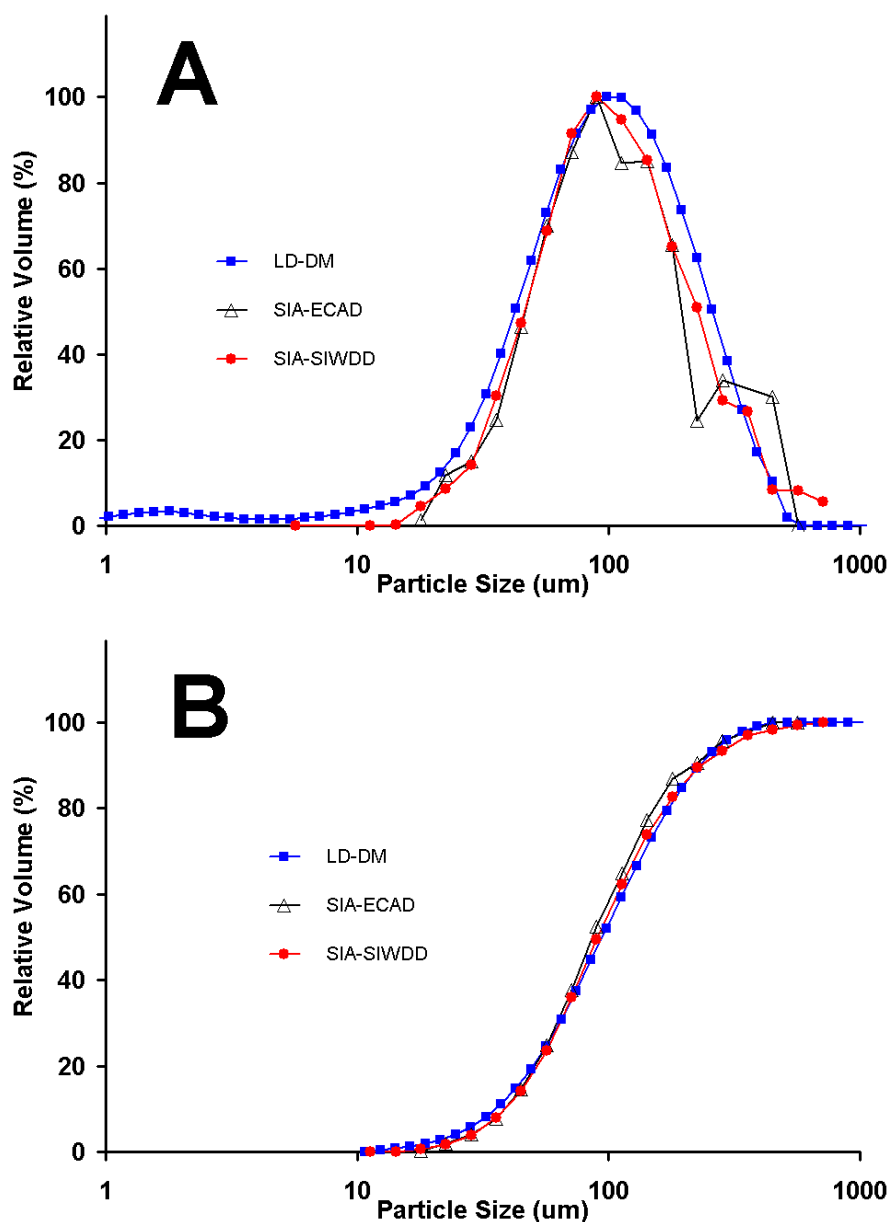
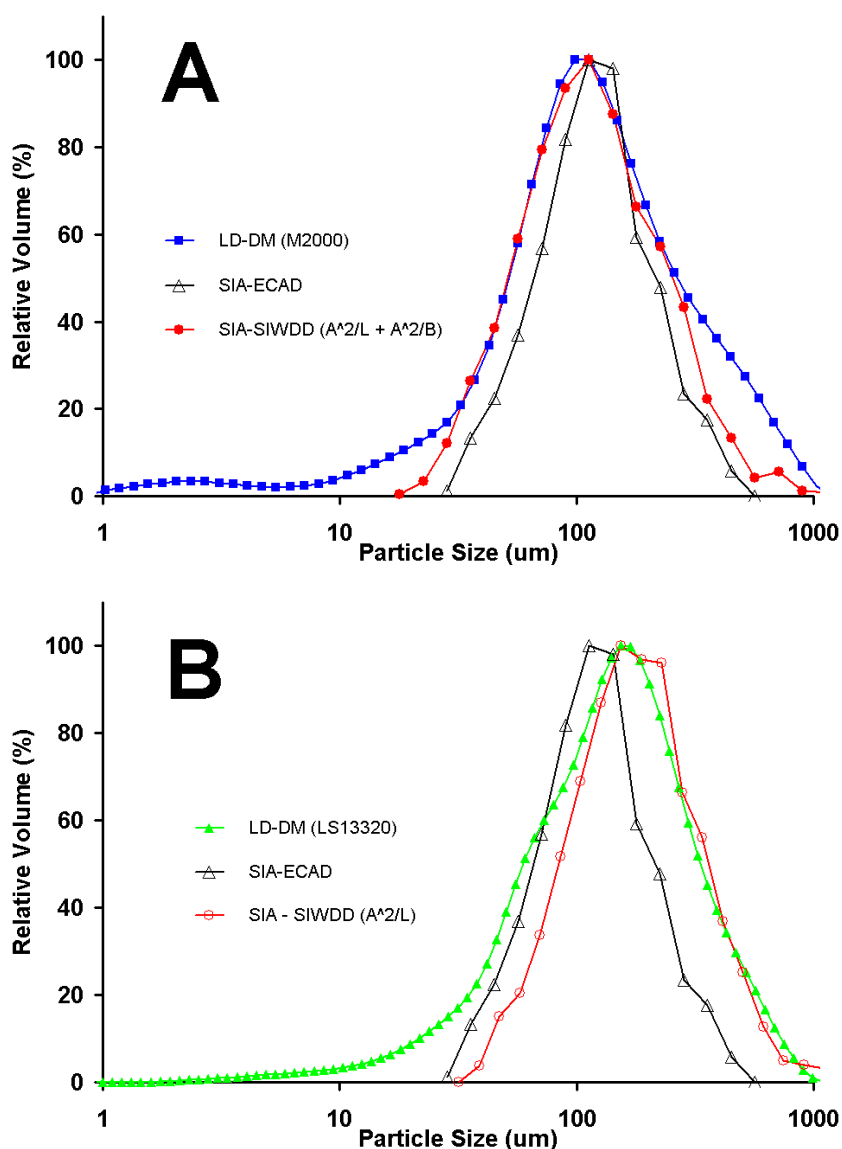


Figure 15

Particle size distribution by volume for Compound H analysed by means of (M2000) a Malvern Mastersizer 2000 laser diffractometer in combination with a Hydro 2000 wet dispersion module in water, (LS13320) a Beckman-Coulter LS13320 laser diffractometer in combination with an ULM wet dispersion module in water, and static image analysis at a 2× magnification and 0.05 bar dispersion pressure, and based on the (SIA-ECAD) equivalent circular area diameter, and (SIA-SIWDD) scattering intensity weighted diffraction diameter of the particles ($A^2/L + A^2/B$ and A^2/L), respectively.



REFERENCES

- 1 United States Pharmacopeia, USP30-NF25, General Chapter <776>, Optical Microscopy.
- 2 B.Y. Shekunov, P. Chattopadhyay, H.H.Y. Tong, A.H.L. Chow. Particle Size Analysis in Pharmaceuticals: Principles, Methods and Applications, Pharmaceutical Research, 24 (2007) 203-227
- 3 A.P. Tinke, R. Govoreanu, K. Vanhoutte. Particle Size and Shape Characterization of Nano- and Submicron Liquid Dispersions, American Pharmaceutical Review, 9 (2006) 33-37.
- 4 A.P. Tinke, K. Vanhoutte, F. Vanhoutte, M. De Smet, H. De Winter. Laser diffraction and image analysis as a supportive analytical tool in the pharmaceutical development of immediate release direct compression formulations, International Journal of Pharmaceutics, 297 (2005) 80-88.
- 5 A. Jillavenkatesa, S.J. Dapkunas, L.S.H. Lum. NIST Recommended Practise Guide, Special Publication 960-1, Particle Size Characterization, Chapter 6: Size Characterization by Laser Light Diffraction Techniques, (2001).
- 6 H. Muhlenweg, E.D. Hirleman. Laser Diffraction Spectroscopy: Influence of Particle Shape and a Shape Adaptation Technique, Particle and Particulate System Characterization, 15 (1998) 163-169.
- 7 C. Heffels, D. Heitzmann, E.D. Hirleman, B. Scarlett. Forward light scattering for arbitrary shap-edged convex crystals in Fraunhofer and anomalous diffraction approximations, Applied Optics, 34 (1995) 6552-6560.
- 8 M. Born and E. Wolf. Principles of Optics: Electromagnetic Theory of Propagation, Interference and Diffraction of Light, Cambridge University

- Press (Cambridge, U.K.), 7th edition. Chapter 8: Elements of the theory of Diffraction, (1997).
- 9 J.W. Goodman. Introduction to Fourier Optics, McGraw-Hill Publishers (Boston, U.S.A.), 2nd edition, Chapter 4: Fresnel and Fraunhofer Diffraction (1996).
 - 10 J. Gebhart. Response of Single-Particle Optical Counters to Particles of Irregular Shape, Particle and Particulate System Characterization, 8 (1991) 40-47.
 - 11 D.W. Schuerman, R.T. Wang, B.A.S. Gustafson, R.W. Schaefer. Systematic studies of light scattering, 1: Particle shape. Applied Optics, 20 (1981) 4039-4050.
 - 12 H.C. Van de Hulst. Light Scattering by Small Particles, Dover Publications Inc., New York, U.S.A., (1957).
 - 13 D.J. Brown, K. Alexander, J. Cao. Anomalous Diffraction Effects in the Sizing of Solid Particles in Liquids, Particle and Particulate System Characterization, 8 (1991) 175-178.
 - 14 A. Beekman, D. Shan, A. Ali, S. Ward-Smith, M. Goldenberg. Micrometer-scale particle sizing by laser diffraction: critical impact of the imaginary component of refractive index, Pharmaceutical Research, 22 (2005) 518-522.
 - 15 F.M. Etzler. Particle Size Analysis: A Comparison of Methods, American Pharmaceutical Review, 7 (2004) 104-108.
 - 16 F. Michel, M.P. Gregoire, E. Pirard. Size distribution of powders in the reange 1 μm – 100 μm : a comparison of static digital image analysis and laser diffraction, Proceedings PARTEC 2007, International Congress on Particle Technology, Nurnberg (Germany), (2007).

- 17 F.M. Etzler, R. Deanne. Particle Size Analysis: A Comparison of Various Methods II, Particle and Particulate System Characterization, 14 (1997) 278-282.
- 18 B.H. Kaye, D. Alliet, L. Switzer, C. Turbitt-Daoust. The Effect of Shape on Intermethod Correlation of Techniques for Characterizing the Size Distribution of Powder. Part 1: Correlating the Size Distribution Measured by Sieving, Image Analysis, and Diffractometer Methods, Particle and Particulate System Characterization, 14 (1997) 219-224.
- 19 H.J. Zhang, G.D. Xu. The effect of particle refractive index on size measurement, Powder Technology, 70 (1992) 189-192.
- 20 B.H. Kaye, D. Alliet, L. Switzer, C. Turbitt-Daoust. The Effect of Shape Characterizing the Size Distribution of Powder. Part 2: Correlating the Size Distribution as Measured by Diffractometer Methods, TSI-Amherst Aerosol Spectrometer, and Coulter Counter, Particle and Particulate System Characterization, 16 (1999) 266-273.
- 21 H. Kanerva, J. Kiesvaara, E. Muttonen, J. Yliruusi. Use of Laser Light Diffraction in Determining the Size Distributions of Different Shaped Particles, Pharmazeutische Industrie, 55 (1993) 849-853.
- 22 C.M.G. Heffels, P.J.T. Verheijen, D. Heitzmann, B. Scarlett. Correction of the Effect of Particle Shape on the Size Distribution Measured with a Laser Diffraction Instrument, Particle and Particulate System Characterization, 13 (1996) 271-279.
- 23 S. Endoh, Y. Kuga, H. Ohya, C. Ikeda, H. Iwata. Shape estimation of anisometric particles using size measurement techniques, Particle and Particulate System Characterization, 15 (1998) 145-149.

- 24 H. Kanerva, J. Kisvaara, E. Muttonen, J. Yliruusi. Evaluation of the Capability of Laser Light Diffraction to Determine the Size Distributions of Spherical Particles, *Pharmazeutische Industrie*, 55 (1993) 775-779.
- 25 A.M. Neumann, H.J.M. Kramer. A Comparative Study of Various Size Distribution Measurement Systems, *Particle and Particulate System Characterization*, 19 (2002) 17-27.
- 26 L. Pieri, M. Bittelli, P.R. Pisa. Laser diffraction, transmission electron microscopy and image analysis to evaluate a bimodal Gaussian model for particle size distribution in soils, *Geoderma*, 135 (2006) 118-132.
- 27 G. Eshel, G.J. Levy, U. Mingelgrin, M.J. Singer. Critical Evaluation of the Use of Laser Diffraction for Particle-Size Distribution Analysis, *Soil Science Society of America Journal*, 68 (2004) 736-743.
- 28 F.M. Etzler, M.S. Sanderson. Particle Size Analysis: a Comparative Study of Various Methods, *Particle and Particulate System Characterization*, 12 (1995) 217-224.
- 29 P. Bowen, C. Vaussourd, H. Hofmann, M. Schellhammer. Accuracy of Particle Size Distribution Measurement of Spherical Glass Beads, *Recent Progres en Genie des Procedes*, 15 (2001) 129-134.
- 30 C. Andres, P. Reginault, M.H. Rochat, B. Chaillot, Y. Pourcelot. Particle-size distribution of a powder: comparison of three analytical techniques, *International Journal of Pharmaceutics*, 144 (1996) 141-146.
- 31 United States Pharmacopeia, USP30-NF25, General Chapter <429>, Light Diffraction Measurement of Particle Size.
- 32 C.M. Barreiros, P.J. Ferreira, M. Figueiredo. Calculating Shape Factors from Particle Size Data, *Particle and Particulate System Characterization*, 13 (1996) 368-373.

- 33 P. Bowen, J. Sheng, N. Jongen. Particle size distribution of anisotropic – particles cylinders and platelets – practical examples, *Powder Technology*, 128 (2002) 256-261.
- 34 M. Li, D. Wilkinson, K. Patchigolla. Comparison of Particle Size Distributions Measured Using Different Techniques, *Particle Science and Technology*, 23 (2005) 265-284.
- 35 U. Tuzun, F.A. Farhadpour. Comparison of Light Scattering with other Techniques for Particle Size Measurement, *Particle Characterization*, 2 (1985) 104-112.
- 36 G.T. Vickers. The projected areas of ellipsoids and cylinders, *Powder Technology*, 86 (1996) 195-200.
- 37 B.R. Jennings and K. Parslow. Particle size measurement: the equivalent spherical diameter, *Proceedings of the Royal Society of London, A* 419 (1998) 137-149.
- 38 N. Gabas, N. Hiquily, C. Laguerie. Response of Laser Diffraction Particle Sizer to Anisometric Particle, *Particle and Particulate System Characterization*, 11 (1994) 121-126.
- 39 T. Matsuyama, H. Yamamoto, B. Scarlett. Transformation of Diffraction Pattern due to Ellipsoids into Equivalent Diameter Distribution of Spheres, *Particle and Particulate System Characterization*, 17 (2000) 41-46.
- 40 R.N. Kelly, J. Kazanjian. Commercial Reference Shape Standards Use in the Study of Particle Shape Effect on Laser Diffraction Particle Size Analysis, *AAPS Pharmaceutical Science Technology*, 7(2) (2006) E1-E12.
- 41 R.N. Kelly, K.J. DiSante, E. Stranzl, J.A. Kazanjian, P. Bowen, T. Matsuyama, N. Gabas N. Graphical Comparison of Image Analysis and

- Laser Diffraction Particle Size Analysis Data Obtained From the Measurements of Nonspherical Particle Systems, *AAPS Pharmaceutical Science Technology*, 7(3) (2006) E1-E14.
- 42 ISO 13322-1:2004(E), Annex A. Particle Size Analysis – Image Analysis Methods – Part 1: Static Image Analysis Methods, (2004).
- 43 A.J. Paine. Error Estimates in the Sampling From Particle Size Distributions, *Particle and Particulate System Characterization*, 10 (1993) 26-32.
- 44 E. Vigneau, C. Loisel, M.F. Devaux, P. Cantoni. Number of particles for the determination of size distribution from microscopic images, *Powder Technology*, 107 (2000) 243-250.
- 45 B.S. Choi, T.A. Ring. Stabilizing NaCl particles with Cd²⁺ in a saturated solution during ex situ PSD measurement, *Journal of Crystal Growth*, 269 (2004) 575-579.
- 46 U. Kohler, J. List, W. Witt. Comparison of Laser Diffraction and Image Analysis under Identical Dispersing Conditions, *Proceedings PARTEC 2007, International Congress on Particle Technology, Nurnberg (Germany)*, (2007).
- 47 C. Berthold, W. Pabst, K.G. Nickel. Influence of detector geometries of common laser diffractometers on the apparent particle size distribution of strongly anisometric particles. *Proceedings of World Congress on Particle Technology 5, Orlando (Florida, U.S.A.), WCPT5 (2006)*.
- 48 R. Xu, O. Andreina Di Guida, Particle Size and Shape Analysis Using Light Scattering, Coulter Principle, and Image Analysis. *Proceedings of World Congress on Particle Technology 4, Sydney (Australia), WCPT4 (2002)*.

- 49** P. Bowen, R. Humphry-Baker, C. Herard. PSD Measurements of Regular Anisotropic Particles – Cylinders and Platelets. Proceedings of World Congress on Particle Technology 3, Brighton (U.K.), WCPT3 (1998).